PNNL-12181
UC-2030

Thermal and Radiolytic Gas Generation Tests on Material from Tanks 241-U-103, 241-AW-101, 241-S-106, and 241-S-102: Status Report

C. M. King
S. A. Bryan

June 1999

Prepared for
the U.S. Department of Energy
under Contract DE-ACO6-76RLO 1830

Pacific Northwest National Laboratory
Richland, Washington 99352

DISCLAIMER

DISCLAIMER

Portions of this document may be illegible in electronic image products. Images are produced from the best available original document.

Executive Summary

This report summarizes progress in evaluating thermal and radiolytic flammable gas generation in actual Hanford single-shell tank wastes. The work described was conducted at Pacific Northwest National Laboratory (PNNL)[a] for the Flammable Gas Safety Project, whose purpose is to develop information to support DE&S Hanford (DESH) and Project Management Hanford Contract (PHMC) subcontractors in their efforts to ensure the safe interim storage of wastes at the Hanford Site. This work is related to gas generation studies performed by Numatec Hanford Corporation (formerly Westinghouse Hanford Company).

This report describes the results of laboratory tests of gas generation from actual convective layer wastes from Tank 241-U-103 under thermal and radiolytic conditions. Accurate measurements of gas generation rates from highly radioactive tank wastes are needed to assess the potential for producing and storing flammable gases within the tanks. The gas generation capacity of the waste in Tank 241-U-103 is a high priority for the Flammable Gas Safety Program due to its potential for accumulating gases above the flammability limit (Johnson et al. 1997).

The objective of this work was to establish the composition of gaseous degradation products formed in actual tank wastes by thermal and radiolytic processes as a function of temperature. The gas generation tests on Tank 241-U-103 samples focused first on the effect of temperature on the composition and rate of gas generation. Generation rates of nitrogen, nitrous oxide, methane, and hydrogen increased with temperature, and the composition of the product gas mixture varied with temperature.

Arrhenius treatment of the rate data yielded activation parameters for gas generation. The measured thermal activation energies, E_a, were determined to be 91 ± 24 kJ/mol for hydrogen, 108 ± 22 kJ/mol for nitrous oxide, 88 ± 34 kJ/mol for nitrogen, and 156 ± 8 kJ/mol for methane (the uncertainties represent 95% confidence intervals).

The second phase of this work concerned gas generation in the presence of a 36,000 rad/hr (^{137}Cs) external gamma source. The effect of radiation was examined at 40, 60, and 90°C. The best estimates of radiolytic G-values, in molecules per 100 eV, were determined to be 0.0019 ± 0.0003 for nitrous oxide, 0.012 ± 0.003 for nitrogen, and 0.0022 ± 0.0003 for methane. The hydrogen G-value was temperature-dependent: 0.006 at 40°C and 0.017 ± 0.004 at 60°C. This is the third tank studied in which the G-values were found to be temperature-dependent.

The rate of hydrogen generation under tank conditions (28.7°C, 449 R/h, 3.02E6 kg waste) was estimated using the thermal and radiolytic activation parameters for gas generation in actual tank waste. The radiolytic generation rate for hydrogen was determined to be 7.1E-8 mol/kg/day, and the thermal rate was 8.7E-8 mol/kg/day. This translates to a total of 0.48 moles of hydrogen

(a) Pacific Northwest National Laboratory is operated by Battelle for the U.S. Department of Energy under Contract DE-AC06-76RLO 1830.

generated per day from this tank. This is much lower than the 5.3 mol/day steady-state hydrogen generation rate reported by McCain (1998) based on Tank 241-U-103 headspace measurements.

The results of low dose-rate tests on material from Tanks 241-AW-101 and 241-S-106 are also presented. $G(H_2)$ appear to be dose-rate dependent at 60°C. The ratio of low to high dose-rate G-values is 2.1 ± 0.1 for 241-AW-101 material, and 3.0 ± 0.9 for 241-S-106 material. $G(H_2)$ also appears to be temperature-dependent. The ratio of 90°C to 60°C high dose-rate G-values is 3.6 ± 0.7 for 241-AW-101 material, 6 ± 4 for 241-S-106 material, and 4.7 ± 1.2 for 241-U-103 material.

The results of a long-term test on Tank 241-S-102 material maintained at near-tank temperature and dose rate, are also presented. The observed rates agree within experimental error with rates predicted using rate parameters obtained at higher temperatures and dose rates, indicating that rate parameters obtained at higher temperatures and dose rates are applicable to tank conditions.

References

Johnson GD, WB Barton, RC Hill, JW Brothers, SA Bryan, PA Gauglitz, LR Pederson, CW Stewart, and LH Stock. 1997. *Flammable Gas Project Topical Report.* HNF-SP-1193 Rev. 2, Lockheed Martin Hanford Corp., Richland, Washington.

McCain DJ and RE Bauer. 1998. *Results of Vapor Space Monitoring of Flammable Gas Watch List Tanks.* HNF-SD-WM-TI-797 Rev 3, Lockheed Martin Hanford Corp., Richland, Washington.

Contents

Figures

Tables

1.0 Introduction

This report describes the research performed to measure gas generation from actual waste taken from a composite sample representing the entire contents of Tank 241-U-103 (U-103).[a] Results of thermal and radiolytic gas generation from Tank U-103 waste are discussed. Work described in this report is being conducted at Pacific Northwest National Laboratory (PNNL) for the Hanford Tank Waste Safety Flammable Gas Project, whose purpose is to develop information needed to support the interim safe storage of nuclear and chemical wastes at the Hanford Site. This work, requested by DE&S Hanford (DESH), began in FY 1997 and continues into FY 1999.

The gas generation tests on U-103 samples focus first on finding the effects of temperature and second on the effects of irradiation with an external source (^{137}Cs capsule). This work was detailed in the Gas Generation Test Plan submitted to the Flammable Gas Project before gas generation testing began.[b] There were no deviations from the stated test plan.

The tank waste samples and radiation source are contained in a hot cell. Gas measurement equipment is contained in an adjacent hood that is attached to the reaction vessels by small-diameter stainless steel tubing. The tests establish gas generation rates from actual waste samples as a function of temperature with and without irradiation. From these results, thermal activation energies can be calculated that allow gas generation rates to be calculated for other temperatures. G-values for the radiolytic gas generation component are also derived from these data.

To assess the effects of temperature on the gas generation from U-103 samples, experiments were performed in duplicate at three temperatures (60, 90, and 120°C) for a total of six reactions. The effects of radiation on gas generation were assessed by repeating the thermal experiment in the presence of an external ^{137}Cs gamma capsule. The irradiation experiments were performed in duplicate at three temperatures (40, 60, and 90°C). The thermal tests provide activation energies for gas generation (Laidler 1987); the radiolytic experiments provide G-values for gas generation (Spinks and Woods 1990). These parameters allow estimation of gas generation rates of the principal gas components within Tank U-103 under current and future conditions.

Section 2 of this report describes the gas generation samples and the experimental conditions and equipment used for the tests. Section 3 presents the results and a discussion of the gas generation experiments. Section 4 describes the results of low dose-rate experiments on AW-101 and S-106 tank material. Section 5 is a summary, and Section 6 contains the cited references.

(a) Hanford waste tanks are designated with the prefix 241-. In this report, as in common usage, the prefix is omitted.

(b) Bryan SA. 1997. *Test Plan: Actual Tank Waste Gas Generation Testing.* TWSFG98.09, Pacific Northwest National Laboratory, Richland, Washington.

2.0 Experimental Methods for Gas Measurements

Gas generation tests on radioactive tank waste were conducted at PNNL's High-Level Radiochemistry Facility in the 325 Building (325A HLRF). A description of the experimental test conditions is given in Section 2.1. A description of the Tank U-103 test material is given in Section 2.2. The self-dose rate from the radionuclide inventory of Tank U-103 samples was calculated to assess the amount of radiolytically induced gas from internal radiation sources. These calculations are given in Section 2.3.

2.1 Experimental Conditions and Equipment

Gas generation measurements were made using reaction vessels and a gas manifold system similar to those used in earlier studies with simulated waste (Bryan and Pederson 1995) and described in earlier reports detailing work with actual waste (Bryan et al. 1996; King et al. 1997). Each vessel has a separate pressure transducer on the gas manifold line. The entire surface of the reaction system exposed to the waste sample is stainless steel except for a gold-plated copper gasket sealing the flange at the top of the reaction vessel. Figure 1 is a drawing of the reaction vessel showing the placement of the thermocouples within and at various locations on the outside of the reaction vessel. Figure 2 is a schematic diagram of the gas manifold system. Temperatures and pressures are recorded every 10 seconds on a Campbell Scientific CR10 datalogger; an average of the data is taken every 20 minutes and saved in a computer file.

The reaction vessels are cylinders of 304 stainless steel. The reaction space of the vessel is approximately 11/16 in. in diameter and 5½ in. high. Each vessel was wrapped in heating tape and insulated. Two thermocouples were attached to the external body of the reaction vessel, one for temperature control and one for over-temperature protection. Two thermocouples were inserted through the lid. The thermocouple centered in the lower half of the vessel monitors the temperature of the liquid phase; the one centered in the upper half monitors the gas phase temperature within the reaction vessel. The reaction vessels were placed in a hot cell and connected by a thin (0.0058 cm inside diameter) tube to the gas manifold outside the hot cell. A stainless steel filter (60-micrometer pore size, Nupro®) protected the tubing and manifold from contamination. A thermocouple was attached to this filter as well.

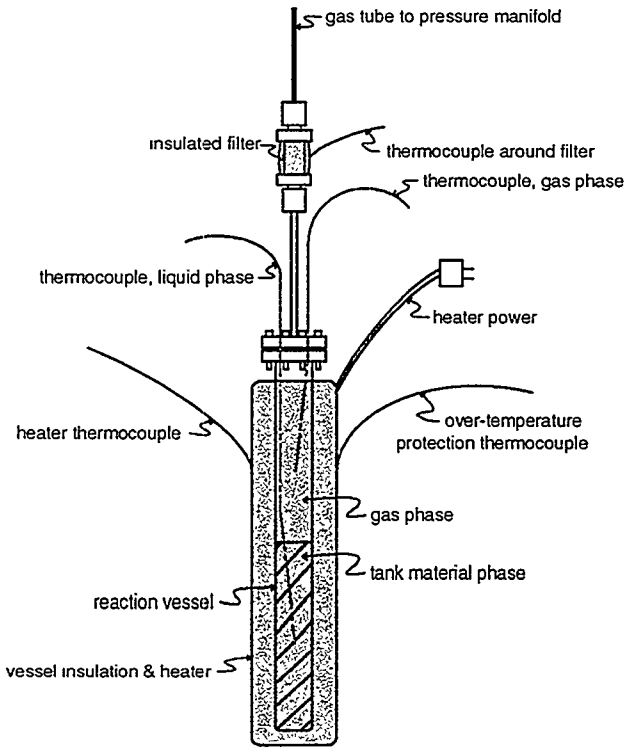

Figure 1. Reaction Vessel Used in Small-Scale Gas Generation Tests

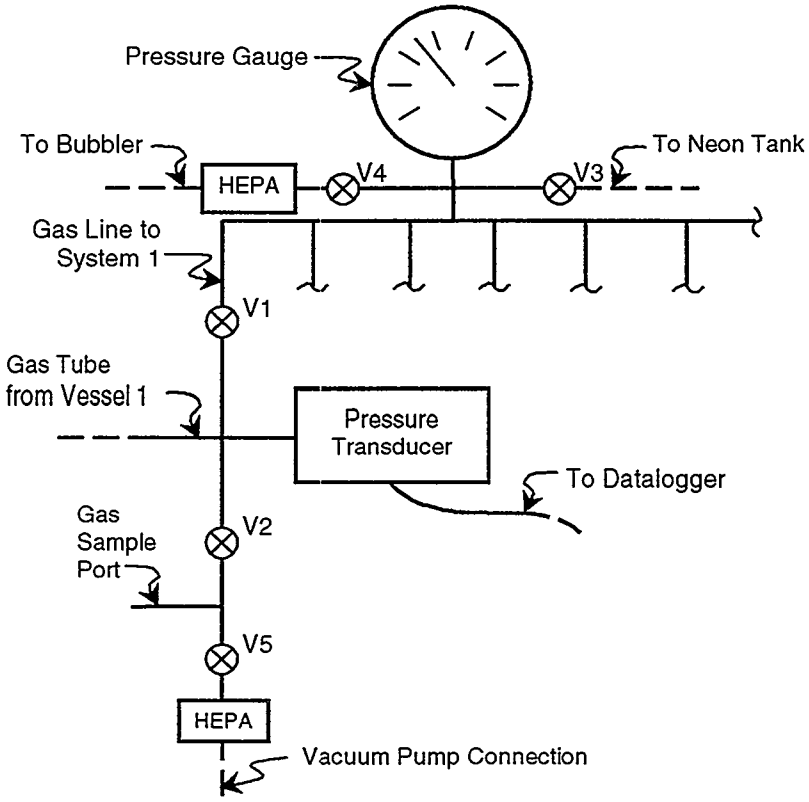

Figure 2. Diagram of Pressure Manifold System Used in Gas Generation Tests

Total moles of gases in the system were calculated using the ideal gas law relationship from the pressure, temperature, and volume of the parts of the apparatus having different gas phase temperatures: $moles_{total} = moles_{vessel} + moles_{filter} + moles_{manifold\ and\ tubing}$. The manifold and filter volumes were determined from pressure/volume relationships using a calibrated gas manifold system. The manifold volume (the pressure sensor, valves, and miscellaneous fittings) was 3.99 mL, the filter volume was 1.34 mL, and the tubing volume was 1.715 mL (by calculation). The cap stem (the tube from vessel to filter) has a volume of 0.20 mL; half of that was added to the filter volume, giving 1.44 mL, and half was added to the vessel volumes. The volume of each vessel was determined gravimetrically by filling it with water. These volumes are recorded in Table 1 along with the mass of waste added to each vessel and the gas phase volume in the vessel after the sample was added. The reproducibility of the molar gas determination using this manifold system has been determined experimentally, and a detailed discussion can be found in Bryan et al. (1996). The relative standard deviation for quantitative gas phase measurements conducted over a time frame similar to that of the gas generation tests was typically less than 2%.

An atmospheric pressure gauge was attached to the datalogger. The pressure in each system is given as the sum of atmospheric pressure and the relative pressure in each system. Neon, because it leaks more slowly than helium from the system, was used as a cover gas. The neon was analyzed independently by mass spectrometry and determined to contain no impurities in concentrations significant enough to warrant correction.

At the start of each run, each system was purged by at least eight cycles of pressurizing with neon at 45 psi (310 kPa) and venting to the atmosphere. The systems were at atmospheric pressure, about 745 mm Hg (99.3 kPa) when sealed. The sample portion of the manifold was isolated (valves V1 and V2 closed) (see Figure 2) for the remainder of the run. The vessels were then heated, adjusting the set points to keep the material within 1°C of the desired liquid phase temperatures. The temperature of the gas phase was 5 to 25°C lower than that of the sample liquid phase.

Table 1. Sample Masses and Vessel Volumes Used In Small-Scale Gas Generation Tests with Tank U-103 Wastes

	Thermal					
System	1	2	3	4	5	6
Temperature, °C	60	60	90	90	120	120
Sample mass, g	30.05	30.00	29.96	30.44	30.68	30.00
Vessel volumes						
gas phase, mL	14.46	14.60	14.39	14.22	14.16	14.46
total, mL	32.50	32.61	32.38	32.50	32.58	32.47
	Radiolytic					
System	7	8	9	10	11	12
Temperature, °C	40	40	60	60	90	90
Sample mass, g	29.96	30.13	29.99	29.87	29.77	29.88
Vessel volumes						
Gas phase, mL	14.53	14.47	14.49	14.58	14.65	14.64
Total, mL	32.52	32.56	32.50	32.51	32.53	32.58

At the end of each run, the vessels were allowed to cool overnight; then a sample of the gas was taken for mass spectrometry analysis. The metal gas collection bottles were equipped with a valve and had a volume of approximately 75 mL (about four times the volume of the gas reaction system). The bottle, after being evacuated overnight at high vacuum, was attached to the gas sample port. Air was removed from the region between valves V2 and V5 (Figure 2) using a vacuum pump, then the gas sample was taken. After the collection bottle was removed, the bottle and sample port were surveyed for radioactive contamination. No contamination was found during these experiments. The reaction vessel was purged again with neon after each sampling event and before the next reaction sequence. For the irradiation experiments, the gamma source was removed from the gas generation apparatus during gas sampling events so that the duration of heating was the same as the duration of irradiation.

Analysis of the composition of the gas phase of each reaction vessel after each run was performed according to analytical procedure PNNL-MA-599 ALO-284 Rev. 1, by staff of the PNNL Mass Spectrometry Facility. The amount of a specific gas formed during heating is given by the mole percent of each gas multiplied by the total moles of gas present in a system. Duplicate samples, which were run in separate reaction vessels and sampled independently at each temperature, were used to assess the reproducibility and uncertainty of the rate parameters.

Gases in the reaction system are assumed to be well mixed, a reasonable assumption. The measured amount of argon in gas samples is an indicator of how much nitrogen from air has leaked into the system (the N_2:Ar ratio in air is 83.6:1). The nitrogen produced in the vessel is the total nitrogen minus atmospheric nitrogen.

The solubilities of nitrogen, hydrogen, methane, and nitrous oxide gases have been measured on simulated waste systems similar in composition to the liquid in U-103 waste (Pederson and Bryan 1996). Less than 0.01% of these gases dissolves in the condensed phase, so loss of these gases due to solubility is negligible.

2.2 Tank U-103 Test Material

The Tank Waste Remediation System Characterization program obtained core samples from Tank U-103. This single-shell tank contains mainly saltcake, with some liquid on the top and sludge on the bottom (Sasaki 1998) (see Figure 3). Best-basis estimates of volumes are given in Table 2.

The average temperature of the tank material from December 23, 1995 to December 23, 1998 was 28.7°C, with a standard deviation of 1.4°C. The best-basis inventory estimate of total organic carbon (TOC) in this tank is 24,300 kg (0.85 wt% carbon in the tank material); the engineering-based inventory estimate of oxalate is 27,500 kg (0.25 wt% oxalate as carbon). Core samples were taken during January and April of 1997. Some of the segments were sent to the 325A HLRF and combined into a composite sample using the amounts shown in Table 3 (segments 1 and 2, and 5 and 6 of core 182 had been combined before being delivered to the HLRF). The density of this composite was calculated to be 1.66 g/mL by taking a weighted average of the densities of the segments. The material was passed through a screen to remove solid chunks larger than about 1/8 in. (0.3 cm) across, then mixed in a single container to obtain homogeneity. The composite had the consistency of wet, runny mud (Figures 4 and 5).

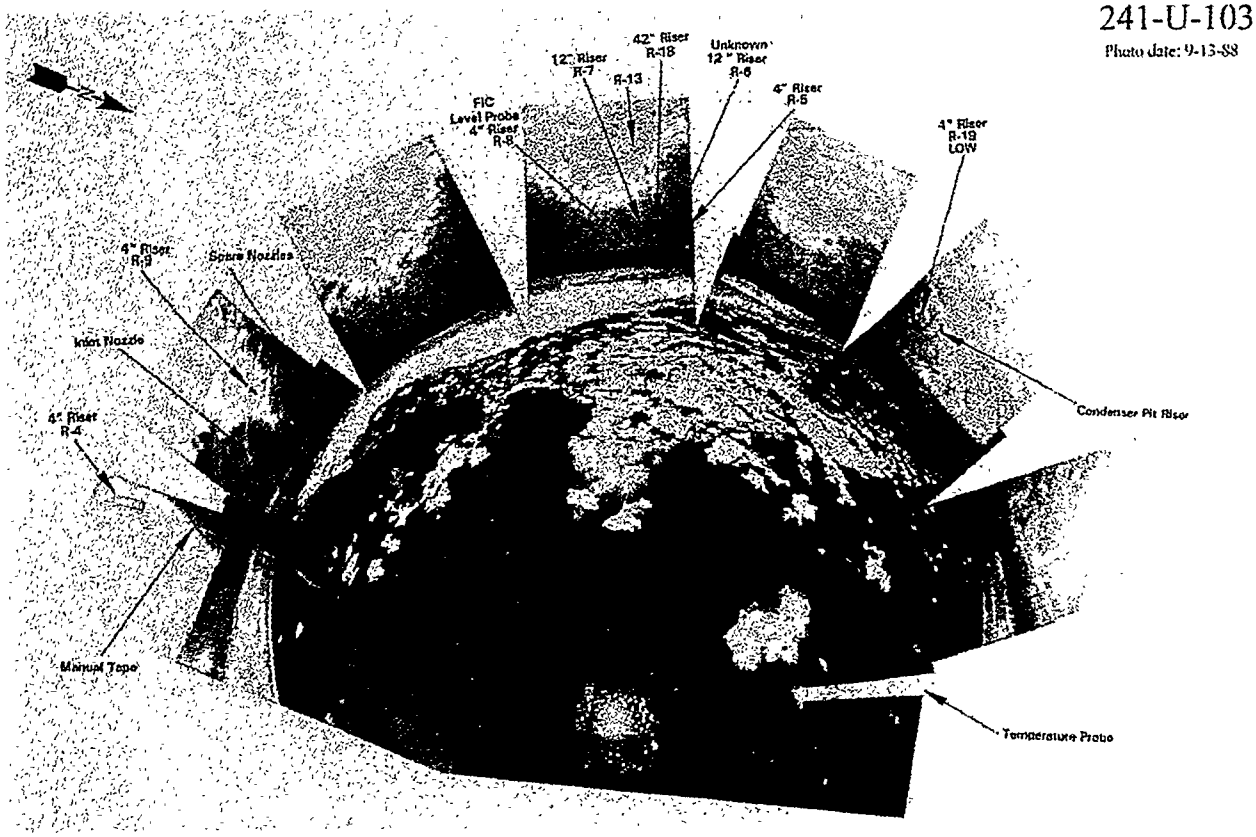

Figure 3. View of Interior of Tank U-103 (the black is the supernatant on top of the saltcake)

Table 2. Tank U-103 Properties (Sasaki 1998)

	Volume, kL	Density, g/mL	Mass, kg
Supernatant	49	1.42	0.07×10^6
Saltcake	1675	1.71	2.86×10^6
Sludge	47	1.9	0.09×10^6
Total	1771		3.02×10^6

Table 3. Material from Cores Used to Prepare U-103 Composite Sample for Gas Generation Tests (distance from top of segment to bottom of tank)

Core	Segments	Distance to bottom of tank, m	Mass used, g
182	1, 2	4.34	69
182	5, 6	2.41	47
176	3	2.93	76
176	5	1.96	96
176	7	1.00	96
176	9	.03	96
		Total:	479

Figure 4. Photo of Homogenized U-103 Material in a Glass Jar Taken with a Digital Camera Inside the Hot Cell Using Incandescent Light

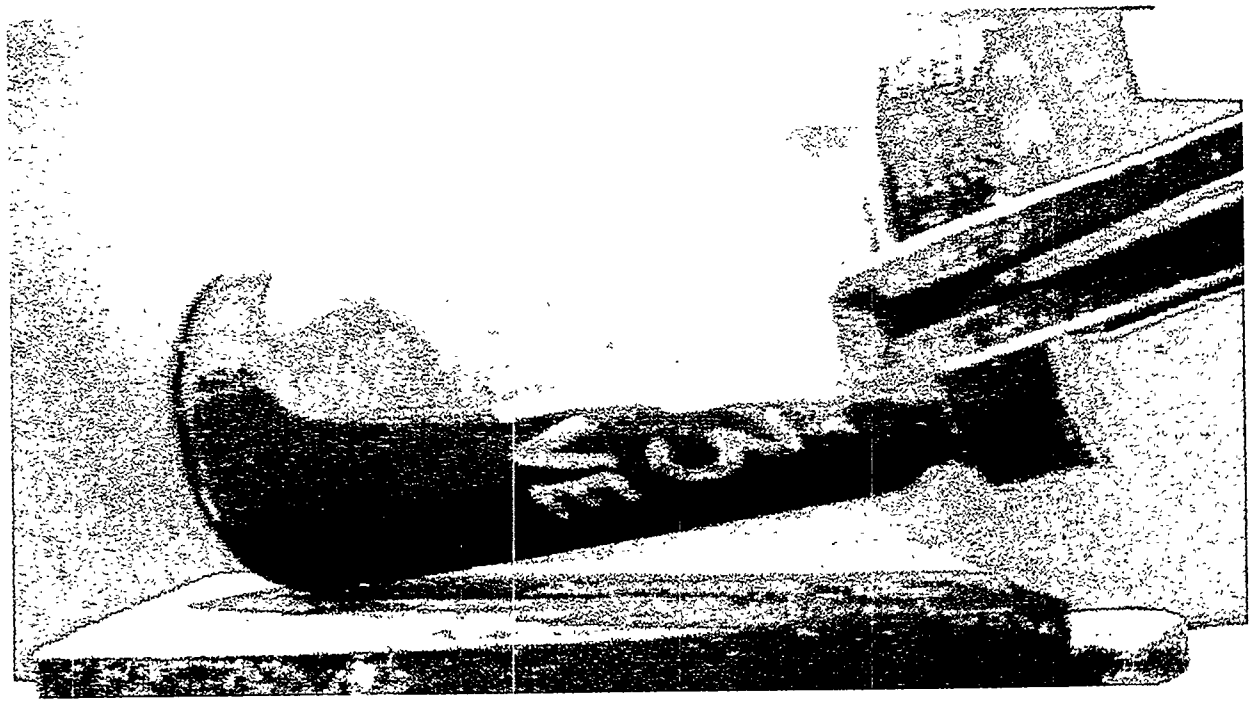

Figure 5. Homogenized U-103 Material Separated over Several Months into a Thick Mud, on the Left, and a Runny Liquid, on the Bottom

2.3 Self-Dose Rate from Radionuclide Inventory in Tank U-103 Samples

The dose rate was calculated for Tank U-103 material both when in the tank and when in a reaction vessel. The dose rate in the tank was calculated from the "best basis" radionuclide inventory for Tank U-103 (Sasaki 1998), assuming that all radiation emitted in the tank is absorbed in the tank. Of course, some of the radiation emitted from the edges of the tank will escape, but this has been shown to be a small amount of the total radiation.[a] The main radionuclides present are $^{137}Cs/^{137m}Ba$ (778,000 Ci), $^{90}Sr/^{90}Y$ (542,000 Ci), ^{151}Sm (21,900 Ci), and ^{154}Eu (1130 Ci). The main sources of alpha radiation are ^{241}Am (193 Ci), ^{239}Pu (161 Ci), ^{240}Pu (27 Ci), ^{238}Pu (4.7 Ci), and ^{238}U (1.1 Ci).

The dose rate in a reaction vessel was calculated by the Dosimetry Research and Technology Group of PNNL using MCNP version 4B (Monte Carlo N-Particle Transport Code System) (Briesmeister 1997). This program uses the Monte Carlo method, in which radiation is emitted in random directions from random locations in the sample. The probabilities of the radiation being either absorbed or scattered by the sample and of its being reflected from the container wall back into the sample are known. Input to the program includes the composition of the walls, the composition of the bulk of the sample, and the radionuclides present. The output is the amount of radiation absorbed by the sample averaged over the entire sample. The reaction vessel was modeled as a cylinder with 1.27-mm-thick steel walls, an inside diameter of 1.73 cm, and a height of 13.97 cm but filled to only a height of 8.5 cm.

The total dose rates averaged over the entire volumes were 449 R/h in the tank and 278 R/h in the vessel. For comparison, the total dose rate in Tank SY-103 was calculated to be 444 R/h (Bryan et al. 1996). The alpha, beta, and gamma components of these values are listed in Table 4. In our past reports, the beta dose rate has been the same in both the vessel and the tank because we have assumed that all of the beta radiation is absorbed by the tank material, whether in the tank or in the vessel. However, some of the energy from beta radiation will be deposited in the container walls rather than in the tank material. The extent of energy loss to the wall was estimated by dividing the material in a vessel into concentric cylinders and calculating the beta dose rate in each cylinder. The calculated dose rate falls off near the wall of the vessel, as shown in Figure 6. However, the volume-average dose rate, 268 R/h, is only 7% less than the beta dose rate in the tank.

The dose rate in a reaction vessel with the ^{137}Cs capsule placed in the middle of the vessel holder was determined by Fricke dosimetry, as described in King et al. (1997). The dose rate received from the ^{137}Cs capsule by the solution within the reaction vessel was 37,400 R/h (average of five determinations) with a relative standard deviation of 6%. That measurement was made 1.65 years before the present gas generation measurements. Correcting for the half-life of ^{137}Cs gives a dose rate during the gas generation measurements of 36,000 R/h.

(a) Bryan SA, CM King, LR Pederson, and SV Forbes. 1996. *Thermal and Radiolytic Gas Generation from Tank 241-SY-103 Waste: Progress Report.* TWSFG96.17, PNNL, Richland, Washington.

Table 4. Calculated Self-Dose Rates in R/h in Tank U-103 and in the Test Vessel

	Gamma	Beta/Electron	Alpha	Total
Tank	160	287	1.5	449
Vessel	8.5	268	1.5	278

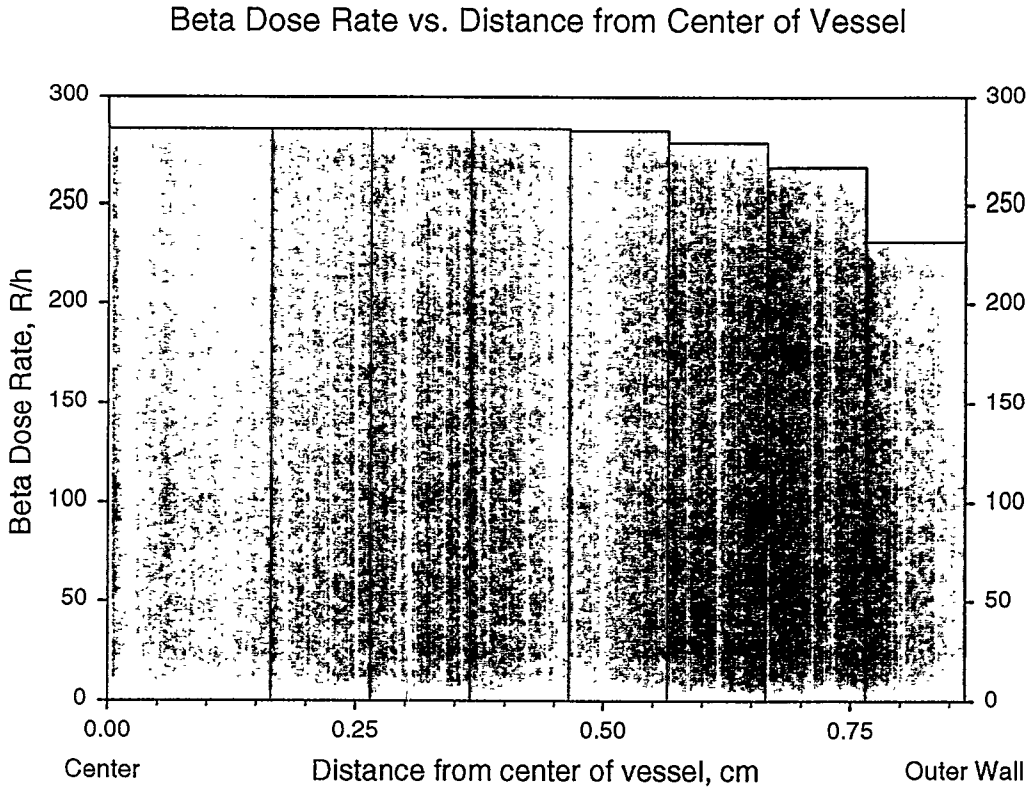

Figure 6. Dropoff of Beta Dose Rate near the Wall of the Reaction Vessel

3.0 Gas Generation from Tank U-103 Waste Samples

Hanford tank waste produces gas as a function of the thermal and radiolytic aging of its components. To assess the relative contributions of thermal and radiolytic components, gas generation was measured from Tank U-103 material under both thermal and radiolytic conditions. By isolating and measuring these components of gas generation, we can predict the gas generation behavior of the waste under current tank conditions or new conditions that may arise over time.

The percent composition and generation rates for gas generation under thermal conditions and radiolytic conditions are described in Section 3.1. Thermal activation parameters from standard Arrhenius treatment of the thermal experiments and G-value determinations from the radiolytic experiments are reported in Section 3.2. Predicted gas generation rates in U-103 under tank conditions and a comparison of gas generation parameters in various tanks are presented in Section 3.3.

3.1 Composition and Rates of Gas Generation from Tank U-103 Waste

Two sets of measurements were made on Tank U-103 material, one in the presence and one in the absence of external radiation. These are referred to as radiolytic and thermal measurements, respectively. Section 3.1.1 presents the thermal results, and Section 3.1.2 presents the radiolytic results. The measurements were run in duplicate at three temperatures, requiring six reaction vessels for each set of measurements. The thermal measurements were made at 60, 90, and 120°C. The radiolytic measurements were made at 40, 60, and 90°C. (The thermal reaction swamps the radiolytic reaction at 120°C, which prevents radiolytic rates from being observed at that temperature.) Each vessel was loaded with the Tank U-103 composite. Gas samples were taken from the vessels periodically. After each gas sample was taken, the vessel was purged to remove previously generated gases before resuming gas generation. Gas generation rates were determined for each gas sample from the heating time, the percent composition of the gas, the total moles of gas in each system when the sample was taken, and from the mass of tank material present in each reaction vessel.

In the tables of percent composition and rates, a run number and a letter identify the reaction vessel and the gas-sampling event, respectively. For example, entries for runs 1a and 2a give data at the first gas-sampling event for vessels 1 and 2, which happen to be duplicates at 60°C.

3.1.1 Thermal Gas Generation from Tank U-103 Waste

This section contains the thermal gas generation data produced by heating material in duplicate reaction vessels at 60, 90, and 120°C in the absence of external radiation. Two samples of the thermally generated gases were taken from each of the six reaction vessels.

The total amount of gas produced versus heating time was calculated for all six reaction vessels (see Figure 7). The rates of gas generation increase with temperature. At 120°C the rate decreases with time (the plots are curved), indicating that gas precursors—presumably organic species—are being consumed.

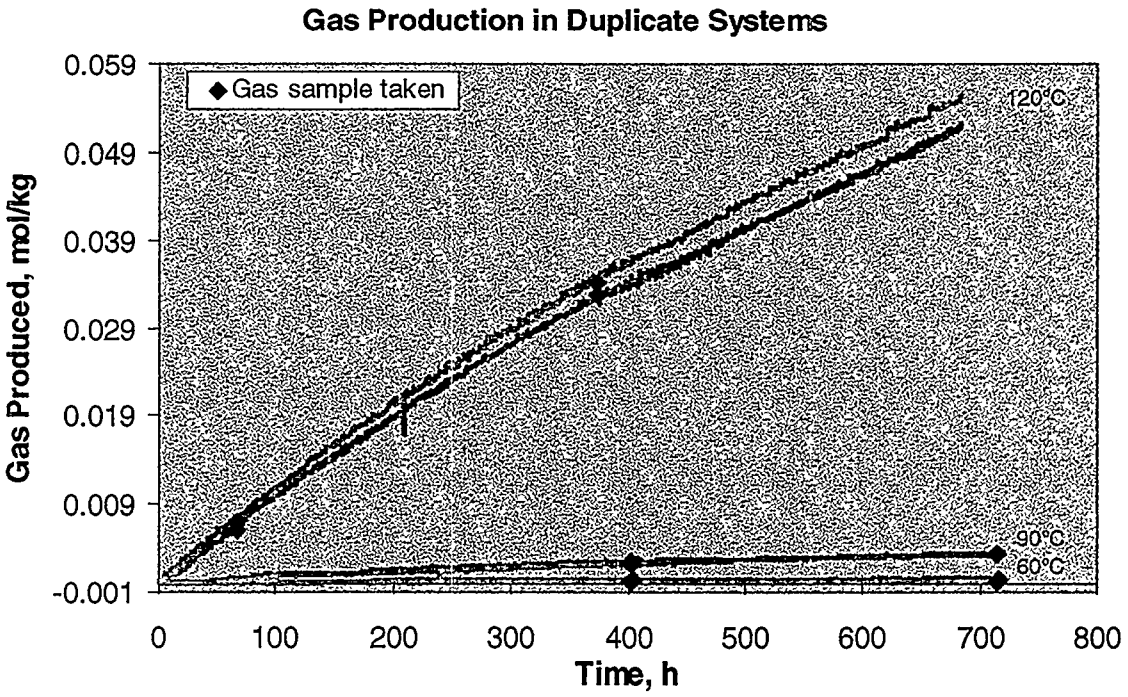

Figure 7. Total Gas Generation from U-103 Material in Reaction Vessels in the Absence of External Radiation. The duplicate runs are indistinguishable at 60 and 90°C.

To obtain separate rates for each gas present, gas samples were analyzed by mass spectrometry. The mole percent composition of these gas samples is given in Table 5. Of more interest is the composition of gas that is generated; this composition is presented below the entry in that table for each run and is shaded. The composition of gas formed during heating is derived from the composition of sampled gas by excluding the neon cover gas, argon, nitrogen from atmospheric contamination, and oxygen. For example, if analysis found 80% neon, 15% nitrous oxide, and 5% hydrogen, the composition of gas formed by excluding neon would be 75% N_2O and 25% H_2. The uncertainties in all the entries in this table are approximately plus or minus one in the last digit.

Argon was used as an indicator of atmospheric contamination because it was not present in the cover gas and was not produced from the waste. Any nitrogen present could have been generated by the waste or could have come from atmospheric contamination. The percent nitrogen actually generated is given by the percent nitrogen found minus 83.6 times the percent argon in the sample (the ratio of nitrogen to argon in dry air is 83.6). The uncertainty in the argon values of approximately 0.001 translates to an uncertainty of 0.08 in the percent nitrogen produced. The argon-corrected percent nitrogen in the runs at 60°C is only about 50% higher than this value. The rate of oxygen generation cannot be determined by the present experiment because tank material consumes oxygen when it is heated (Person 1996). The uncertainty in the argon values translates to an uncertainty of 0.02 in the percent oxygen produced. The percent oxygen found in the samples was always less than this value and often negative, indicating that it was indeed being consumed.

Table 5. Mole Percent Composition of Thermal Gas Sampled (including Ne) and Formed (shaded), and Heating Times of Duplicate Systems at Three Temperatures (no external radiation source was used for these samples)[a]

	Mole Percent of Gas Formed at 60°C										
Run	Ne	Ar	N_2	H_2	N_2O	CH_4	O_2	NH_3[b]	NO_x	$C_2H_{2,4,or\,6}$	Time, h
1a	99.5	0.002	0.208	0.183	0.037	0.004	0.031			0.002	404
			36	32	14	1.1				6	
1b	99.5	0.003	0.28	0.145	0.029	0.005	0.020				311
			39	50	10	1.7					
2a	98.9	0.008	0.73	0.212	0.046	0.004	0.056			0.002	403
			55	32	11	1.0				5	
2b	99.5	0.003	0.28	0.139	0.036	0.005	0.026				311
			39	47	12	1.7					
	Mole Percent of Gas Formed at 90°C										
Run	Ne	Ar	N_2	H_2	N_2O	CH_4	O_2	NH_3[b]	NO_x	$C_2H_{2,4,or\,6}$	Time, h
3a	97.0	0.002	0.76	1.42	0.37	0.32	0.029			0.011	403
			24	51	13.2	11.4				39	
3b	98.1	0.002	0.66	0.59	0.32	0.25	0.027			0.004	311
			33	34	18.3	14				2	
4a	97.6	0.003	0.63	1.10	0.41	0.24	0.017			0.009	404
			21	49	18.4	10.8				40	
4b	98.5	0.003	0.52	0.41	0.34	0.13	0.048		0.027	0.004	311
			28	32	27	10			2.1	3	
	Mole Percent of Gas Formed at 120°C										
Run	Ne	Ar	N_2	H_2	N_2O	CH_4	O_2	NH_3[b]	NO_x	$C_2H_{2,4,or\,6}$	Time, h
5a	90.4	0.002	2.22	3.73	1.57	2.05	0.012		0.011	0.020	66
			22.4	39	16.5	21.5			12	21	
5b	55.1	0.002	7.6	12.9	11.7	12.1	0.016	0.5		0.030	307
			16.8	29	26	27		1		067	
6a	89.2	0.002	2.45	4.07	1.83	2.290	0.016	0.1	0.018	0.022	66
			22.1	38	17.1	21.9		9	17	21	
6b	54.6	0.002	7.5	13.2	12.1	11.9	0.017	0.5	0.03	0.030	307
			16.4	29	27	26		1	07	066	

(a) Blank entries are below detection limits.

(b) Measurements for ammonia are for the gas phase only and do not include ammonia dissolved in the liquid phase.

Ammonia concentrations in the gas phase above the samples were also measured by mass spectrometry (Table 5). A large fraction of ammonia is expected to remain in the liquid phase (Pederson and Bryan 1996). The sum of all percents for a run may not be exactly 100 because of rounding and because traces of hydrocarbons other than $C_2H_{2,4,or\,6}$ found in some samples are omitted from Table 5.

The mole percent composition for the initial gas samples at each temperature is shown graphically in Figure 8. The most notable trend is the increase in percent methane with temperature; the percent hydrogen decreased slightly with temperature. Using the percent composition data, reaction times, and mass of each sample, rates of gas generation were determined. These rates are given in Table 6 as a function of temperature.

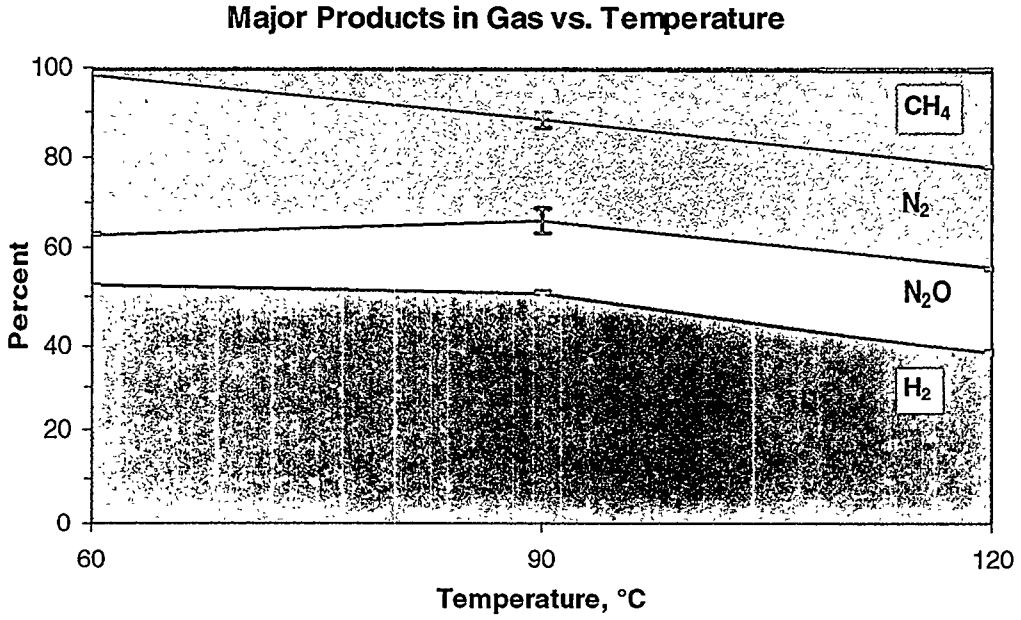

Figure 8. Percent Composition of Major Gas Products from Thermal Reactions of U-103 Waste as a Function of Temperature. Error bars give the range of duplicate samples.

Table 6. Gas Generation Rates from Thermal Treatment of Tank U-103 Material in the Absence of an External Radiation Source

			60°C Gas Generation Rates, mol/kg/day						
Run	N_2	N_2O	H_2	NH_3[(a)]	NO_x	CH_4	$C_2H_{2,4,or\,6}$	Other HC[(b)]	Total
1a	2.2E-6	6.5E-7	3.2E-6			7.0E-8	3.5E-8		6.1E-6
1b	2.5E-6	6.4E-7	3.2E-6			1.1E-7			6.5E-6
2a	2.5E-6	8.0E-7	3.7E-6			7.0E-8	3.5E-8		7.1E-6
2b	2.5E-6	8.1E-7	3.1E-6			1.1E-7			6.6E-6

			90°C Gas Generation Rates, mol/kg/day						
Run	N_2	N_2O	H_2	NH_3[(a)]	NO_x	CH_4	$C_2H_{2,4,or\,6}$	Other HC[(b)]	Total
3a	1.3E-5	7.1E-6	2.7E-5			6.2E-6	2.1E-7	2.7E-8	5.4E-5
3b	1.4E-5	7.6E-6	1.4E-5			5.9E-6	9.5E-8	1.2E-7	4.1E-5
4a	8.7E-6	7.7E-6	2.1E-5			4.5E-6	1.7E-7	2.4E-8	4.2E-5
4b	8.0E-6	7.7E-6	9.3E-6		6.1E-7	2.9E-6	9.1E-8	1.1E-7	2.9E-5

			120°C Gas Generation Rates, mol/kg/day						
Run	N_2	N_2O	H_2	NH_3[(a)]	NO_x	CH_4	$C_2H_{2,4,or\,6}$	Other HC[(b)]	Total
5a	2.8E-4	2.1E-4	5.0E-4		1.5E-6	2.7E-4	2.7E-6	2.7E-7	1.3E-3
5b	3.1E-4	4.8E-4	5.2E-4	2.0E-5		4.9E-4	1.2E-6	1.6E-7	1.8E-3
6a	3.3E-4	2.5E-4	5.6E-4	1.4E-5	2.5E-6	3.2E-4	3.0E-6	2.8E-7	1.5E-3
6b	3.1E-4	5.1E-4	5.6E-4	2.1E-5	1.3E-6	5.0E-4	1.3E-6	1.7E-7	1.9E-3

(a) Ammonia measurements are for gas phase only and do not include ammonia dissolved in the liquid phase.

(b) Hydrocarbons.

3.1.2 Radiolytic Gas Generation from Tank U-103 Waste

This section contains the data from producing gases radiolytically by placing a ^{137}Cs source (gamma capsule) next to the reaction vessels while heating the material in the reaction vessels to temperatures of 40, 60, and 90°C. Two gas samples were taken from each of the six reaction vessels. A leak developed in the vessel used for the 40°C runs 8a and 8b; data from that vessel were not used in deriving rate parameters.

The total amount of gas produced versus heating time was calculated for all five reaction vessels (Figure 9). The rates of gas generation increase with temperature.

The mole percent composition of the gas sampled at the end of each run is given in Table 7. No ammonia was detected in these runs. (In the thermal runs ammonia was only detected at 120°C.) The rates of gas generation obtained from each runs are given in Table 8.

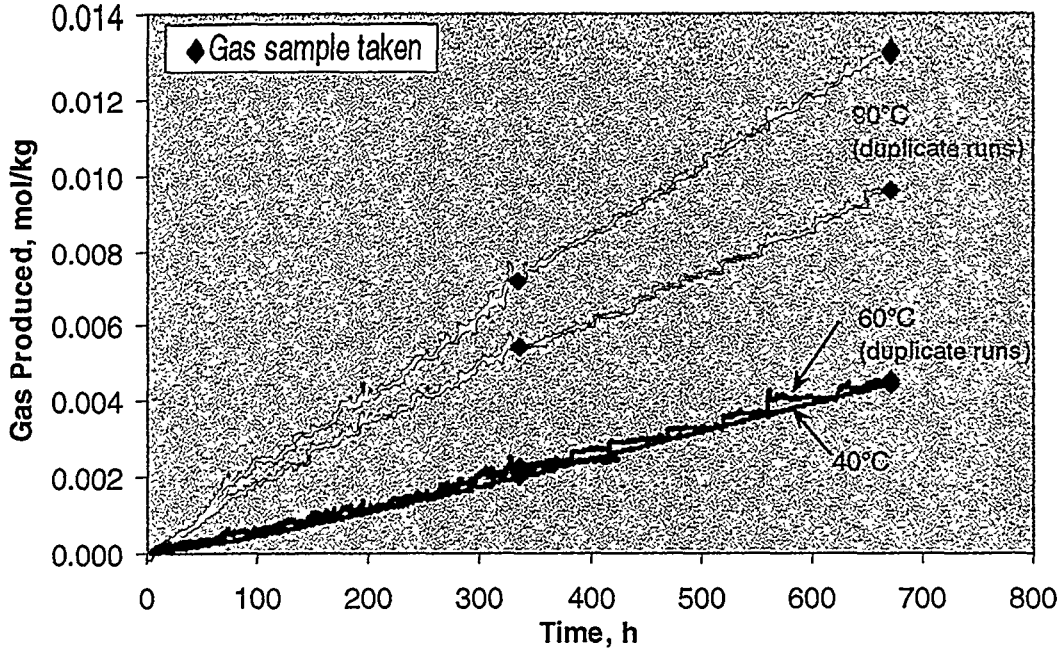

Figure 9. Total Gas Generation from U-103 Material in Reaction Vessels in the Presence of 37,400 R/h External Radiation. A thermocouple malfunction prevents displaying one of the duplicate 60°C runs beyond about 425 hours.

3.2 Thermal and Radiolytic Rate Parameters for Gas Generation from Tank U-103 Waste

The three most important mechanisms for gas generation from waste have been determined to be 1) radiolytic decomposition of water and some organic species; 2) thermally driven chemical reactions, mainly involving organic complexants and solvents; and 3) chemical decomposition of the steel tank walls (Johnson et al. 1997). The total gas generation rate is the sum of the radiolytic, thermal, and corrosion rates:

$$\text{Total Rate} = \text{Radiolytic Rate} + \text{Thermal Rate} + \text{Corrosion Rate} \quad (1)$$

Table 7. Mole Percent Composition of Radiolytic Gas Sampled (including Ne) and Formed (shaded) and Heating Times of Duplicate Systems at Three Temperatures (external radiation source used for these samples)[a]

Mole Percent of Gas Formed at 40°C

Run	Ne	Ar	N_2	H_2	N_2O	CH_4	O_2	NO_x	$C_2H_{2,4,\text{ or }6}$	Time, h
7a	97.7	0.007	0.97	0.273	0.79	0.078	0.128	0.015		336
			28.8	16.8	49	4.8		9		
7b	95.8	0.009	1.52	0.55	1.89	0.069	0.129		0.006	335
			26.7	55	14.9	4			2	
8a	50.4	0.44	38.8	0.43	1.62	0.11	8.1	0.030	0.010	336
			49	10.0	38	2.6		70	2	
8b	37.1	0.56	49	0.377	2.29	0.070	10.7		0.011	335
			45	7.5	46	1.4			2	

Mole Percent of Gas Formed at 60°C

Run	Ne	Ar	N_2	H_2	N_2O	CH_4	O_2	NO_x	$C_2H_{2,4,\text{ or }6}$	Time, h
9a	97.1	0.003	0.88	0.95	0.86	0.101	0.042	0.015	0.006	336
			27	36	33	3.8		6	2	
9b	95.0	0.004	1.54	1.64	1.58	0.12	0.056		0.006	335
			27.8	35	34	2.6			1	
10a	95.4	0.004	0.69	0.67	0.63	0.085	0.095		0.006	336
			24	37	34	4.6			3	
10c	96.1	0.006	1.09	1.02	1.19	0.070	0.093		0.006	335
			23	34	40	2.4			2	

Mole Percent of Gas Formed at 90°C

Run	Ne	Ar	N_2	H_2	N_2O	CH_4	O_2	NO_x	$C_2H_{2,4,\text{ or }6}$	Time, h
11a	91.4	0.004	2.04	4.5	1.34	0.45	0.035	0.012	0.013	336
			22.1	56	16.5	5.6		1	2	
11b	90.8	0.002	1.36	4.8	1.45	0.50	0.038		0.008	335
			15.9	60	18.0	6.2			10	
12a	91.7	0.004	1.90	3.79	0.86	0.41	0.042	0.014	0.011	336
			24.5	56	12.8	6.1		2	2	
12b	92.6	0.003	1.05	3.53	0.88	0.34	0.057		0.008	335
			15.6	63	15.6	6.0			1	

(a) Blank entries are below detection limits. Uncertainties are ±1 in the last digit.

Because radiolytic and thermal rates dominate (Johnson et al. 1997), they are the focus of these experiments. The thermal rate varies with temperature. The relation between thermal rate constants, k, at different temperatures is given by the Arrhenius equation:

$$k = Ae^{\left(\frac{-E_a}{RT}\right)} \tag{2}$$

where R is the gas constant, 8.314 J/K-mol, T is the temperature in Kelvin, E_a is the activation energy, and A is the pre-exponential factor. The initial thermal rate is assumed to be zero order,

Table 8. Gas Generation Rates from Radiolytic Treatment of Tank U-103 Material in the Presence of an External Radiation Source

			40°C Gas Generation Rates, mol/kg/day						
Run	N_2[a]	N_2O	H_2	NH_3[b]	NO_x	CH_4	$C_2H_{2,4,or6}$	Other HC[c]	Total
7a	1.0E-5	1.8E-5	6.1E-6		3.3E-7	1.7E-6			3.6E-5
7b	1.9E-5	4.2E-5	1.2E-5			1.5E-6	1.3E-7		7.5E-5
8a	4.2E-5	3.2E-5	8.5E-6		6.0E-7	2.2E-6	2.0E-7		8.5E-5
8b	4.6E-5	4.7E-5	7.7E-6			1.4E-6	2.2E-7		1.0E-4

			60°C Gas Generation Rates, mol/kg/day						
Run	N_2[a]	N_2O	H_2	NH_3[b]	NO_x	CH_4	$C_2H_{2,4,or6}$	Other HC[c]	Total
9a	1.6E-5	1.9E-5	2.1E-5		3.4E-7	2.3E-6	1.4E-7		6.0E-5
9b	2.9E-5	3.5E-5	3.7E-5			2.7E-6	1.3E-7		1.0E-4
10a	9.9E-6	1.4E-5	1.5E-5			1.9E-6	1.3E-7	4.5E-8	4.1E-5
10b	1.5E-5	2.6E-5	2.3E-5			1.6E-6	1.3E-7	2.2E-8	6.6E-5

			90°C Gas Generation Rates, mol/kg/day						
Run	N_2[a]	N_2O	H_2	NH_3[b]	NO_x	CH_4	$C_2H_{2,4,or6}$	Other HC[c]	Total
11a	5.3E-5	4.0E-5	1.3E-4		3.5E-7	1.3E-5	3.8E-7	5.9E-8	2.4E-4
11b	3.7E-5	4.2E-5	1.4E-4			1.4E-5	2.3E-7	5.7E-8	2.3E-4
12a	4.2E-5	2.2E-5	9.6E-5		3.6E-7	1.0E-5	2.8E-7	5.1E-8	1.7E-4
12b	2.1E-5	2.1E-5	8.5E-5			8.2E-6	1.9E-7	4.8E-8	1.4E-4

(a) The nitrogen rates are corrected for atmospheric contamination using argon percent minus 0.001%.
(b) Ammonia measurements are for gas phase only and don't include that dissolved in the liquid phase.
(c) Hydrocarbons.

in which case the rate constant is equivalent to the observed rate. Plots of the observed gas generation, Figures 7 and 9, show that gas generation is essentially linear up to the first gas sample. Data from the linear (initial) portion of each product versus time curve was used as a measure of the initial rate of the reaction. A plot of moles of gas produced versus time would be linear for a zero-order rate law, and the portion of the data used in the kinetic treatment falls under pseudo-zero-order conditions. That is, at initial times in the reaction progress, concentrations of reagents are essentially unchanged. Only at later times and for the higher temperature reactions do the rates lower due to the consumption of reactive components within the waste samples. Values of E_a and A can then be determined from the rates measured in the reaction vessels. The equation allows the thermal rates to be calculated at temperatures at which the rate is so slow that it is difficult to measure directly.

The radiolytic rate at a given temperature is determined experimentally by measuring the difference between rates measured in the presence and absence of external radiation. The G-value, a dose-independent rate, is related to the radiolytic rate by Equation 3:

$$\text{G-value(molecules/100 eV)} = \frac{\text{Radiolytic rate (mol/kg/day)}}{\text{Dose rate (R/hr)}} \times (4.02 \times 10^7) \qquad (3)$$

The constant 4.02 x 10^7 is a unit conversion factor. Because the radiolytic rate is calculated from the difference of two experimental rates, its 95% confidence interval is given by

$$\sigma_{radiolytic} = \sqrt{\sigma^2_{thermal} + \sigma^2_{thermal+radiolytic}}$$

The 95% confidence interval for the thermal rates is easily obtained from the thermal data. The 95% confidence interval rates measured in the presence of external radiation is not available so it is estimated, at a given temperature, as half the range of the duplicate measurements. Radiolytic rates have been observed to be temperature independent in both water radiolysis and in the radiolytic rates measured in Tank SY-103 material. However, temperature-dependent rates were observed in Tank U-103 material.

The experimental thermal and radiolytic rates for hydrogen, nitrous oxide, nitrogen, and methane generation, represented by symbols, are shown in Figure 10 (rates from the second gas sample are omitted). Duplicate runs are distinguished by a dot in the center of the symbols. These dots can be used to detect systematic errors. For example, at 90°C, circles representing the slowest nitrogen and slowest hydrogen thermal rates both contain dots, indicating that both rate measurements were obtained from the same reaction vessel. This observation suggests that the difference between duplicate measurements is partly due to inhomogeneity of the samples. The curved lines in Figure 10 are predicted temperature-independent radiolytic rates, which are thermal rates plus a constant representing a G-value. The G-values derived from this data are listed in Table 9. Included in Table 9 are the thermal parameters for $C_2H_{2,4,or\,6}$; U-103 is the first tank for which G-values could be obtained for the two-carbon hydrocarbons. The G-values appear to be temperature independent for nitrous oxide, nitrogen, and methane generation. The "best" G-value estimate is an average of two 60°C and one 40°C G-value (because of the leak occurring in one of the 40° reaction vessels). The G-value for hydrogen generation appears to be temperature-dependent. As shown in Figure 10, the G-value is different at each temperature.

The G-values were used to correct the thermal runs for self-radiolysis, using the self-radiolysis dose rate of 278 R/h from Section 2.3. A least-squares fit of these thermal-only rates gave the E_a and A parameters in Table 9. Both A and its natural logarithm are given. The 95% confidence interval for E_a and ln(A) is the value plus or minus the number in parentheses. The E_a and A parameters were used to calculate the straight lines in Figure 10. The correlation coefficients for the thermal data corrected for self-radiolysis, R^2 in Table 9, indicate that the thermal data are well described by the Arrhenius relation.

An Arrhenius plot of the thermal gas generation rates for hydrogen, nitrous oxide, nitrogen, and methane, along with activation energies, is shown in Figure 11. Thermally, at 60°C, hydrogen is produced fastest and methane is slowest.

The observed temperature dependence of $G(N_2)$, $G(N_2O)$, and $G(H_2)$ can be explained by the radiolytic generation of intermediates which themselves thermally decompose to gaseous products. Such intermediates include H_2NOH (which decomposes to N_2, N_2O, and NH_3) and formaldehyde and other aldehydes (which decompose to H_2 and carboxylates). The thermal decomposition of these intermediates would be temperature-dependent, even if the initial

Table 9. Thermal and Radiolytic Rate Parameters for Gas Generation from U-103 Waste

	H_2	N_2O	N_2	CH_4
E_a, kJ/mol	91 ± 24	108 ± 22	88 ± 34	156 ± 8
A, mol/kg/day	5.2E+8	3.5E+10	1.0E+8	1.4E+17
ln(A)	20 ± 8	24 ± 7	18 ± 11	40 ± 3
R^2	0.966	0.979	0.929	0.999
G-value at 40°C	0.006	0.019	0.011	0.0019
G-value at 60°C	0.017 ± 0.004	0.018 ± 0.003	0.013 ± 0.003	0.0023 ± 0.0002
G-value at 90°C	0.08 ± 0.02	0.02 ± 0.01	0.029 ± 0.006	0.007 ± 0.002
Best G-value[(a)]	Temperature-dependent	0.019 ± 0.003	0.012 ± 0.003	0.0022 ± 0.0003

	$C_2H_{2,4,or6}$
E_a, kJ/mol	79 ± 21
A, mol/kg/day	7.5E+4
ln(A)	11 ± 7
R^2	0.965
G-value at 60°C	0.00014 ± 0.0001
G-value at 90°C	0.0002 ± 0.0001

(a) Best estimate is obtained by averaging the two 60°C and one 40°C measurements.

radiolytic production of these species was temperature independent. However, some wastes exhibit temperature independent G-values for gas generation. It is possible under certain chemical conditions that gases are formed primarily by direct radiolysis or that the intermediates are short-lived under all temperature conditions measured and therefore do not show observable temperature dependence.

3.3 Calculated Gas Generation Rates for U-103 Waste Under Tank Conditions

The tank conditions are 28.7°C and an average dose rate of 449 R/h. The radiolytic gas generation rates in the tank were calculated using the "best" G-values in Table 9 for nitrogen, nitrous oxide and methane; for hydrogen, the 40°C G-value was used. The thermal gas generation rates were calculated using the thermal parameters in Table 9. These rates are given in Table 10 along with the total generation rate. The rates of gas generation from the entire tank per day are given in Table 11. According to calculations, about 12 L of hydrogen are produced each day from this tank. Gas generation parameters for all the tanks we have examined are compared in Tables 12, 13, and 14. In those tables, the 95% confidence interval is presented as an uncertainty in the last decimal parenthesis: 1.02(3) represents 1.02 ± 0.03.

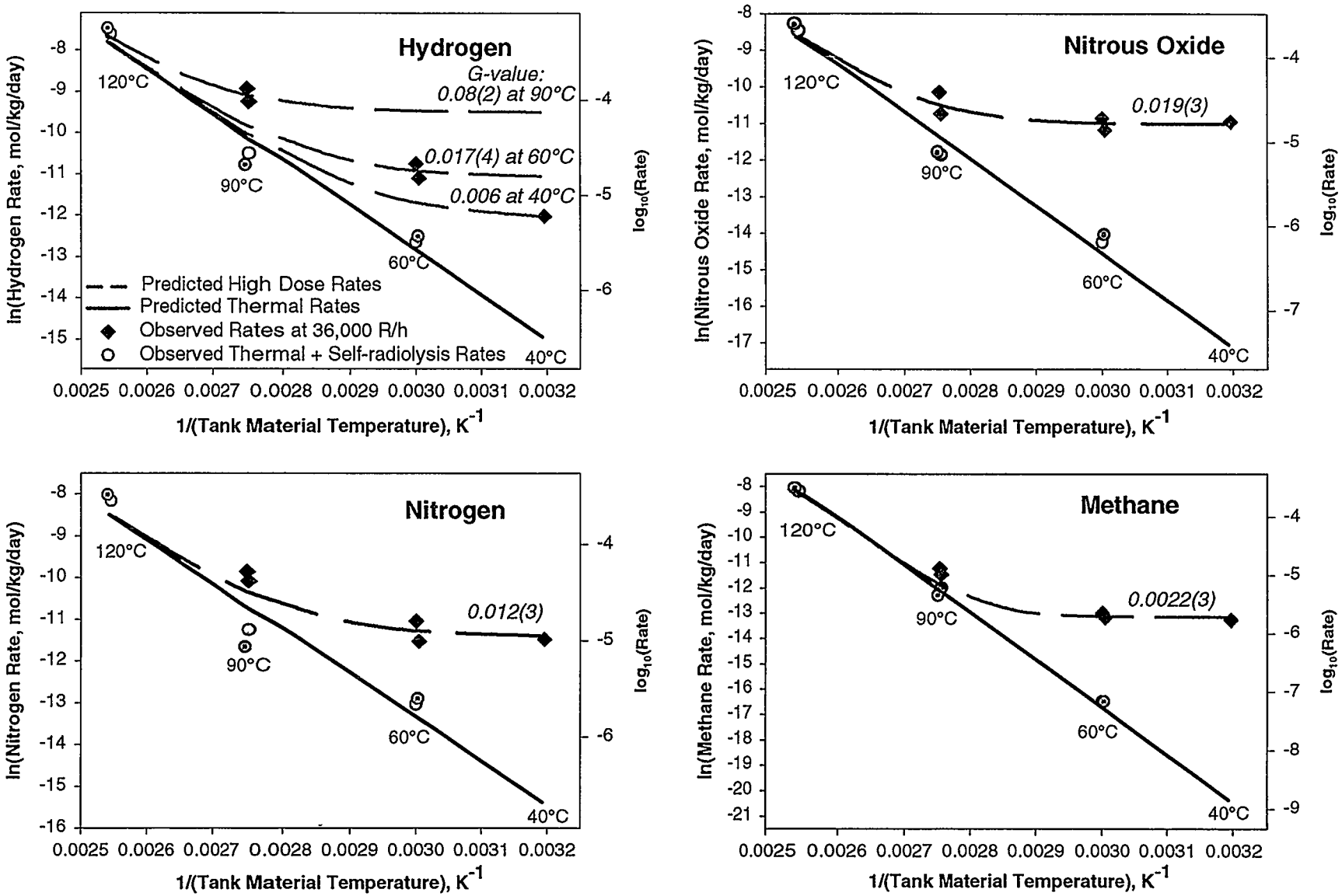

Figure 10. Tank U-103 Gas Generation Rates. The small dot in the center of the symbols distinguishes between duplicate runs.

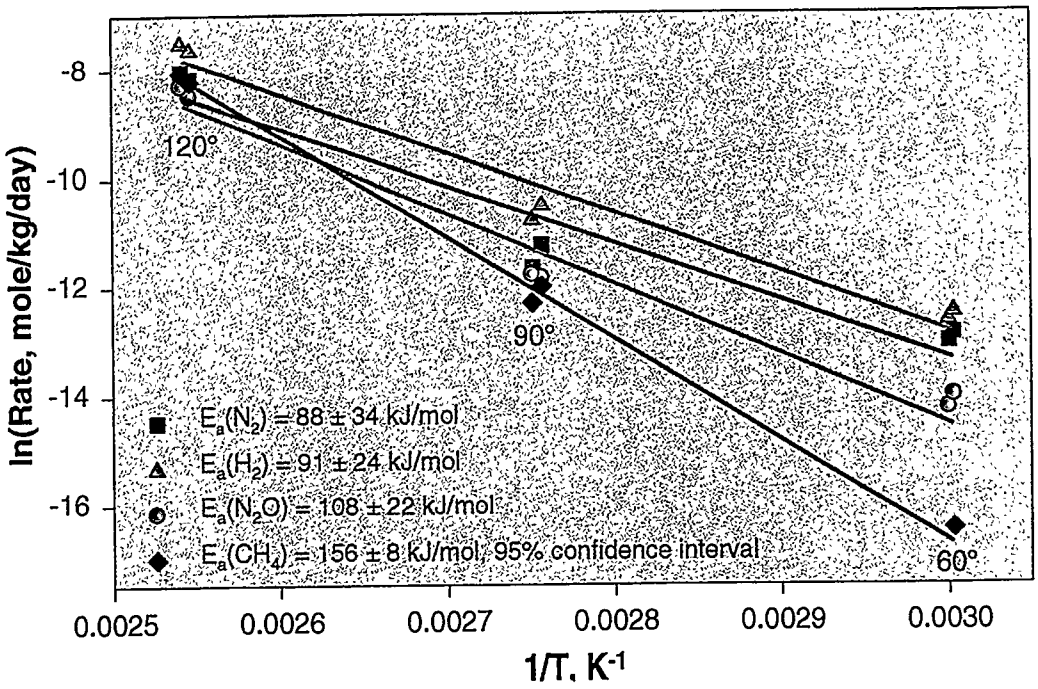

Figure 11. Arrhenius Plot of Thermal U-103 Gas Generation Rate Data Showing Activation Energies

Table 10. Calculated Gas Generation from U-103 at Tank Conditions (449 R/h, 28.7°C)

	Composition,	Rates, mol/kg/day				
	mol %	Total	Radiolytic	Thermal	% Radiolytic	% Thermal
H_2	27	1.6E-7	7.1E-8	8.7E-8	45.1	54.9
N_2O	36	2.2E-7	2.1E-7	8.4E-9	96.1	3.9
N_2	33	2.0E-7	1.4E-7	6.0E-8	69.9	30.1
CH_4	4.1	2.4E-8	2.4E-8	1.6E-10	99.4	0.6

Table 11. Gas Formed Each Day from the Entire Tank under Tank Conditions

	Moles of gas formed per day
H_2	0.48
N_2O	0.65
N_2	0.60
CH_4	0.07

Table 12. Comparison of Gas Generation Parameters[a] in Tanks Previously Tested

	H_2			N_2O			N_2			CH_4		
	E_a	ln(A)	G-value	E_a	ln(A)	G-value	E_a	ln(A)	G-value	E_a	ln(A)	G-value
A-101, top[b]	101(8)	22(3)	0.0051(4)	77(27)	13(9)	0.0038(4)	118(18)	28(6)	0.0020(4)	125(32)	28(10)	0.00021(4)
AW-101,cv[c,d]	102(3)	25(1)	0.101(1)	131(20)	33(7)	0.0189(1)	126(15)	31(5)	0.011(1)	138(6)	33(2)	0.00106(2)
S-102[e]	80(19)	15(6)	0.017(4)	87(7)	17(2)	0.009(3)	65(39)	9(12)	0.010(3)	127(33)	29(11)	0.0005(2)
S-106[f]	73(6)	12(2)	0.0048(6)	62(47)	8(16)	0.00013(8)	95(28)	19(9)	0.0049(4)	104(8)	21(3)	0.00031(3)
SY-103[g],**cv**	91(9)	21(3)	0.14	117(9)	29(3)	0.036	84(10)	17(3)	0.036	146(18)	34(6)	0.003(1)
U-103[h]	91(24)	20(8)	0.006	108(22)	24(7)	0.019(3)	88(34)	18(11)	0.012(3)	156(8)	40(3)	0.0022(3)

(a) Units: Ea, kJ/mol; A, mol/kg/day; G-value, molecules/100 eV. (b) Bryan and King 1998. *Thermal and Radiolytic Gas Generation from Tank 241-A-101 Waste: Status Report.* TWS98.78, PNNL, Richland, Washington. (c) cv = convective layer. (d) Bryan and King 1998. *Thermal and Radiolytic Gas Generation from Tank 241-AW-101 Waste: Status Report.* TWS98.39, PNNL, Richland, Washington. (e) King et al. 1997. (f) King and Bryan 1998. *Thermal and Radiolytic Gas Generation from Tank 241-S-106 Waste: Status Report.* TWS98.78, PNNL, Richland, Washington. (g) Bryan et al. 1996.(h) Results of this study.

Table 13. Comparison of Gas Generation Rates at Tank Conditions in Tanks Previously Tested[a]

	H_2			N_2O			N_2			CH_4		
	Per day	Rad	Thermal	Per day	Rad	Thermal	Per day	Rad	Thermal	Per day	Rad	Thermal
A-101, top	1.13	5.1E-8	3.3E-7	0.73	3.8E-8	2.1E-7	0.59	2.0E-8	1.8E-7	0.06	2.1E-9	1.7E-8
AW-101, cv	10.0	2.0E-6	4.9E-7	1.6	3.7E-7	3.0E-8	1.0	2.1E-7	2.7E-8	0.09	2.1E-8	2.2E-9
S-102	1.0(2)	1.6E-7	8.6E-8	0.4(1)	5E-8	4E-8	0.2(1)	5E-8	6E-9	0.019(4)	2.7E-9	2.2E-9
S-106	0.19	2.1E-8	3.9E-8	0.20	5.7E-10	6.3E-8	0.08	2.2E-8	4.9E-9	0.007	1.4E-9	8.5E-10
SY-103, cv	3.8(5)	1.5(2)E-6	3(2)E-7	0.9(2)	3.6(9)E-7	6(4)E-8	2(1)	1.2(3)E-7	7(4)E-7	0.08	3E-8	4E-11
U-103	0.48	7.1E-8	8.7E-8	0.65	2.1E-7	8.4E-9	0.60	1.4E-7	6.0E-8	0.07	2.4E-8	1.6E-10

(a) Rad: Radiolytic rate. Rad and Thermal rates are in mol/kg/day. Per day rate is in moles from entire tank, or layer.

Table 14. Comparison of Tank Properties

	Temperature, °C	Dose rate, R/h	Wt% Non-oxalate TOC	Mass of tank or layer, kg
A-101, top (saltcake)	58	411	0.24	2.98E+6
AW-101, convective layer	37	786	0.29[a]	4.04E+6
S-102	41	207	0.11	3.95E+6
S-106	25	177	0.14	3.09E+6
SY-103, convective layer	31.7	443	0.74	2.05E+6
U-103	28.7	449	0.60	3.02E+6

(a) Carlson 1997.

4.0 Low Dose-Rate Gas Generation

Previous gas generation measurements on Tanks AW-101 and S-106 raised the possibility that G-values may be dose-rate-dependent. To test that hypothesis, radiolytic gas generation rates were measured at a dose rate of 3564 R/h, which is about 10% of the dose rate used in the original measurements.

4.1 Low Dose-Rate Gas Generation from Tank AW-101 Waste

The test material was liquid from the convective layer of AW-101 (Figure 12).[a] The total gas produced from Tank AW-101 material as a function of time is shown in Figure 13. As usual, the rate decreases with time at 120°C. The spikes in the 120°C runs are attributed to refluxing in the reaction vessels: when a drop of water drips down on top of the hot vessel contents it immediately vaporizes, increasing the moles of gas in the system.

The diamonds in Figure 13 indicate when gas samples were taken. The mole percent composition of these gas samples is given in Table 15, along with the composition of gas that is generated. The AW-101 gas generation rates are listed in Table 16 and are compared in Figure 14. The observed G-values are listed in Table 17.

The methane rates from duplicate runs agree closely. This precision indicates that the samples are homogenous, as expected for liquid samples, and that the uncertainties are small in

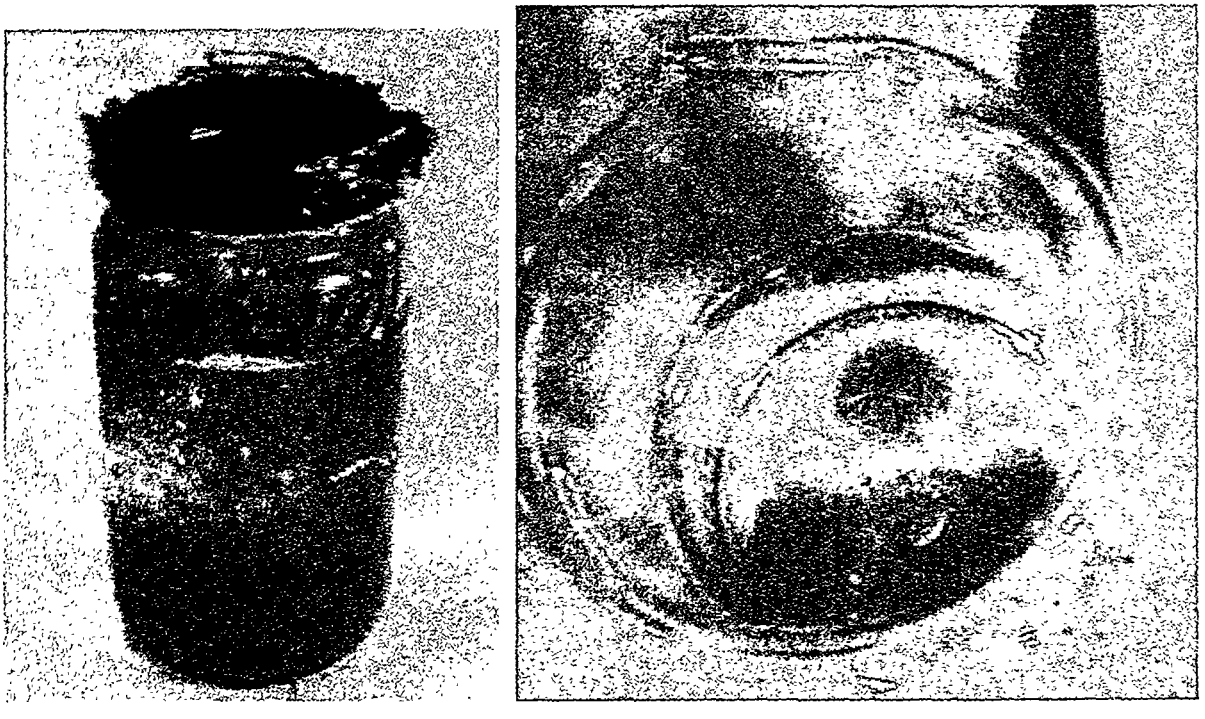

Figure 12. Photos of AW-101 Convective Layer Material

(a) Bryan and King 1998. *Thermal and Radiolytic Gas Generation from Tank 241-AW-101 Waste: Status Report.* TWS98.39, PNNL, Richland, Washington.

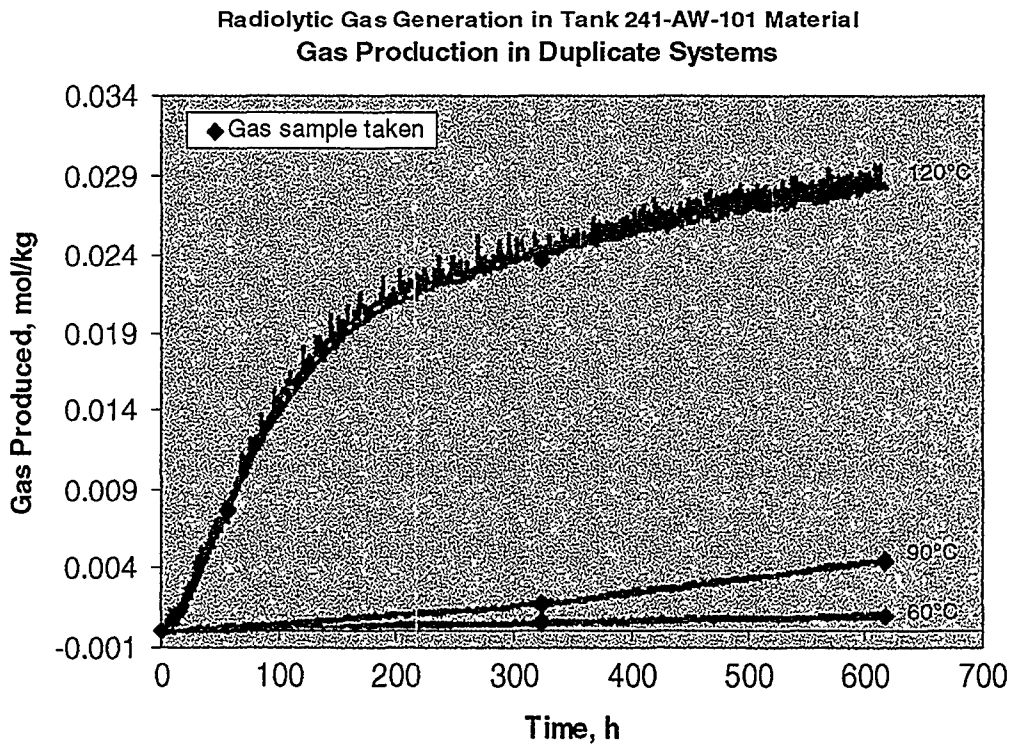

Figure 13. Total Gas Produced in Externally Irradiated AW-101 Material as a Function of Time. The duplicate runs are indistinguishable.

the measured variables of time, sample mass, temperature, moles of gas in the vessel, and percent methane in the gas. At 60°C the low dose rate runs have slower rates than the high dose-rate runs, and faster rates than the thermal + self-radiolysis runs, as expected. The low and high dose-rate G-values at 60°C—0.0015 ± 0.0003 and 0.00106 ± 0.00003, respectively—are observed to be indistinguishable within experimental error, so methane generation rates are assumed to be dose rate independent.

At high dose rate, the ratio of 90°C to 60°C $G(H_2)$ is 3.6 ± 0.7, indicating that $G(H_2)$ is temperature-dependent. A similar ratio of 4.7 ± 1.2 was found in Tank U-103. $G(H_2)$ is also dose-rate dependent; the low-dose 60°C $G(H_2)$ is 2.1 ± 0.1 times as large as the high dose-rate value.

The low-dose and high-dose $G(N_2)$ values do not differ significantly from each other at 60°C; $G(N_2)$ is therefore dose rate-independent. At 90 and 120°C, the radiolytic rates are somewhat less than the thermal rates; this could be random experimental error.

The low- and high-dose $G(N_2O)$ values also do not differ significantly from each other at 60°C; $G(N_2O)$ is therefore dose rate-independent. At 90 and 120°C, the radiolytic rates are considerably less than the thermal rates. No basis has been found for discarding the nitrous oxide rate data, so we conclude that some unidentified process in the reaction vessels reduces the radiolytic rate below the thermal-only rate.

Table 15. Mole Percent Composition of Radiolytic Gas Sampled (including Ne) and Gas Formed (shaded), and Heating Times of Duplicate Systems at Three Temperatures (an external radiation source was used for these samples)[a]

	Mole Percent of Gas Formed at 60°C										
Run	Ne	Ar	N_2	H_2	N_2O	CH_4	O_2	NH_3[b]	NO_x	$C_2H_{2,4,\text{or}\,6}$	Time, h
1a	98.1	0.003	0.26	1.41	0.116	0.012	0.057			0.004	324
			5.7	86	7.1	.7				.2	
1b	98.2	0.004	0.37	1.21	0.102	0.011	0.065			0.003	293
			8.2	84	7.1	.8				.2	
2a	98.1	0.003	0.280	1.44	0.123	0.012	0.076			0.004	324
			6.7	85	7.3	.71				.24	
2b	98.0	0.005	0.43	1.29	0.105	0.010	0.115				293
			6.4	86	7.0	.7					
	Mole Percent of Gas Formed at 90°C										
Run	Ne	Ar	N_2	H_2	N_2O	CH_4	O_2	NH_3[b]	NO_x	$C_2H_{2,4,\text{or}\,6}$	Time, h
3a	92.5	0.003	0.86	5.8	0.43	0.26	0.049			0.044	323
			9.6	80	5.9	3.6				.61	
3b	89.7	0.003	2.24	5.7	1.96	0.22	0.074		0.01	0.007	293
			20.8	57	19.7	2.2			.10	.07	
4a	92.1	0.004	0.78	6.3	0.47	0.25	0.034			0.038	323
			7.0	83	6.2	3.3				.50	
4b	89.7	0.004	2.11	5.90	1.89	0.21	0.112		0.025	0.009	293
			18.8	60	19.1	2.1			.25	.09	
	Mole Percent of Gas Formed at 120°C										
Run	Ne	Ar	N_2	H_2	N_2O	CH_4	O_2	NH_3[b]	NO_x	$C_2H_{2,4,\text{or}\,6}$	Time, h
5a	77.4	0.003	3.85	12.3	5.1	1.28	0.017			0.042	56
			16.4	55	22.7	5.7				.19	
5b	62.5	0.002	8.8	15.0	10.5	2.65	0.020		0.12	0.022	267
			23.5	41	28.4	7.2			.32	.059	
6a	79.1	0.002	3.55	11.6	4.4	1.19	0.038		0.06	0.039	56
			16.7	56	21.2	5.7			.29	.19	
6b	64.8		7.9	14.4	9.9	2.50	0.013		0.11	0.023	267
			22.7	41	28.4	7.2			.32	.066	

(a) Blank entries are below detection limits.

(b) Measurements for ammonia are for the gas phase only and do not include ammonia dissolved in the liquid phase.

Table 16. Gas Generation Rates from Low-Dose Radiolytic Treatment of Tank AW-101 Material

	60°C Gas Generation Rates, mol/kg/day								
Run	N_2	N_2O	H_2	NH_3[(a)]	NO_x	CH_4	$C_2H_{2,4,or\,6}$	Other HC[(b)]	Total
1a	1.8E-6	2.3E-6	2.8E-5			2.3E-7	7.8E-8	2.0E-8	3.2E-5
1b	2.6E-6	2.2E-6	2.6E-5			2.4E-7	6.5E-8		3.1E-5
2a	2.1E-6	2.3E-6	2.6E-5			2.2E-7	7.3E-8	1.8E-8	3.1E-5
2b	1.9E-6	2.1E-6	2.6E-5			2.0E-7			3.0E-5

	90°C Gas Generation Rates, mol/kg/day								
Run	N_2	N_2O	H_2	NH_3[(a)]	NO_x	CH_4	$C_2H_{2,4,or\,6}$	Other HC[(b)]	Total
3a	1.4E-5	8.7E-6	1.2E-4			5.2E-6	8.9E-7	8.1E-8	1.5E-4
3b	4.7E-5	4.4E-5	1.3E-4		2.3E-7	5.0E-6	1.6E-7	2.3E-8	2.3E-4
4a	1.1E-5	9.4E-6	1.3E-4			5.0E-6	7.6E-7	4.0E-8	1.5E-4
4b	4.2E-5	4.2E-5	1.3E-4		5.6E-7	4.7E-6	2.0E-7	4.5E-8	2.2E-4

	120°C Gas Generation Rates, mol/kg/day								
Run	N_2	N_2O	H_2	NH_3[(a)]	NO_x	CH_4	$C_2H_{2,4,or\,6}$	Other HC[(b)]	Total
5a	5.1E-4	7.1E-4	1.7E-3			1.8E-4	5.8E-6	7.0E-6	3.1E-3
5b	3.1E-4	3.8E-4	5.4E-4		4.3E-6	9.5E-5	7.9E-7	1.4E-7	1.3E-3
6a	5.3E-4	6.8E-4	1.8E-3		9.2E-6	1.8E-4	6.0E-6	4.6E-6	3.2E-3
6b	3.0E-4	3.8E-4	5.6E-4		4.2E-6	9.6E-5	8.9E-7	1.5E-7	1.3E-3

(a) Measurements for ammonia are for the gas phase only and do not include ammonia dissolved in the liquid phase.
(b) Hydrocarbons.

Table 17. G-values for Gas Generation from AW-101 Waste

	H_2	N_2O	N_2	CH_4
60°C Low Dose Rate	0.21(1)	0.01(1)	0.012(9)	0.0015(3)
60°C High Dose Rate	0.101(1)	0.019(1)	0.0107(9)	0.00106(3)
90°C High Dose Rate	0.36(7)			

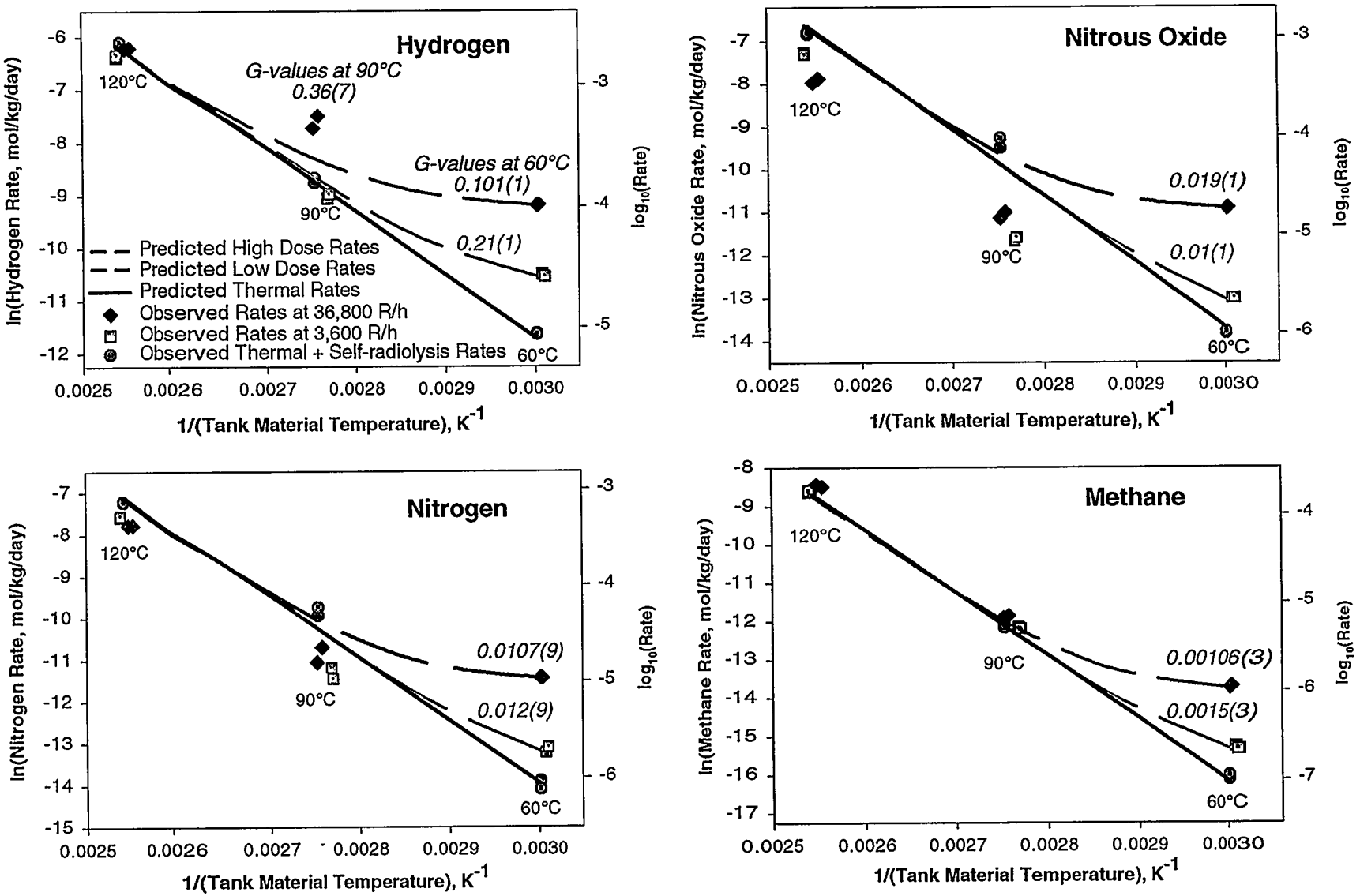

Figure 14. Tank AW-101 Gas Generation Rates. The small dot in the center of the symbols distinguishes between duplicate runs.

4.2 Low Dose-Rate Gas Generation from Tank S-106 Waste

The S-106 test material has been described in an unpublished letter report.[a] The composition of gas generated from S-106 material is given in Table 18. The S-106 gas generation rates are listed in Table 19 and compared in Figure 15. The observed G-values are listed in Table 20.

The rate of methane generation at 120°C appears to be unusually accelerated in the presence of external radiation. The cause of this is not understood. The high- and low-dose G-values at 60°C appear to differ significantly.

Like methane, the rate of hydrogen generation at 120°C appears to be unusually accelerated in the presence of external radiation. $G(H_2)$ appears to be dose rate-dependent: at 60°C, the low dose-rate G-value is 3.0 ± 0.9 times larger than the high dose-rate G-value. $G(H_2)$ is also temperature-dependent: at high-dose rate, the ratio of 90°C to 60°C $G(H_2)$ values is 6 ± 4. The low-dose and high-dose $G(N_2)$ values do differ from each other at 60°C, but the difference is probably not significant; $G(N_2)$ is therefore assumed to be dose rate-independent.

$G(N_2O)$ could not be determined from the nitrous oxide rates due to scatter in the data. However, the gas generation rate appears to slow down when the tank material is exposed to high-dose external radiation.

4.3 Evaluation of Dose-Rate and Temperature Dependence of Hydrogen G-values

$G(H_2)$ appears to be dose-rate dependent at 60°C. The ratio of low to high dose-rate G-values is 2.1 ± 0.1 for AW-101 material and 3.0 ± 0.9 for S-106 material. The difference between these ratios is not statistically significant.

$G(H_2)$ also appears to be temperature-dependent. The ratio of 90°C to 60°C high dose-rate G-values is 3.6 ± 0.7 for AW-101 material, 6 ± 4 for S-106 material, and 4.7 ± 1.2 for U-103 material. The difference between these ratios is also not statistically significant.

(a) King and Bryan 1998. *Thermal and Radiolytic Gas Generation from Tank 241-S-106 Waste: Status Report.* TWS98.78. PNNL, Richland, Washington.

Table 18 Mole Percent Composition of Radiolytic Gas Sampled (including Ne) and Gas Formed (shaded), and Heating Times of Duplicate Systems at Three Temperatures (an external radiation source was used for these samples)[a]

	Mole Percent of Gas Formed at 60°C										
Run	Ne	Ar	N_2	H_2	N_2O	CH_4	O_2	NH_3[b]	NO_x	$C_2H_{2,4,or\,6}$	Time, h
1a	99.4	0.005	0.38	0.058	0.025	0.004	0.128				323
			34	44	19	3					
1b	99.4	0.005	0.40	0.064	0.009	0.004	0.115				293
			46	45	6	3					
2a	99.6	0.002	0.20	0.058	0.035	0.003	0.059				323
			55	27	16	14					
2b	99.6	0.003	0.25	0.070	0.013	0.004	0.077				293
			49	41	7.7	2.4					
	Mole Percent of Gas Formed at 90°C										
Run	Ne	Ar	N_2	H_2	N_2O	CH_4	O_2	NH_3[b]	NO_x	$C_2H_{2,4,or\,6}$	Time, h
3a	99.1	0.002	0.32	0.344	0.047	0.092	0.045				323
			39	48	7	12.8					
3b	99.1	0.002	0.30	0.333	0.100	0.09	0.061				293
			29	45	14	12.2					
4a	99.0	0.003	0.35	0.357	0.096	0.096	0.070			0.003	323
			25	48	13	13.0				.4	
4b	99.2	0.003	0.28	0.337	0.023	0.089	0.052				293
			20	60	4	16					
	Mole Percent of Gas Formed at 120°C										
Run	Ne	Ar	N_2	H_2	N_2O	CH_4	O_2	NH_3[b]	NO_x	$C_2H_{2,4,or\,6}$	Time, h
5a	98.4	0.003	0.44	0.363	0.45	0.28	0.012			0.003	56
			19.9	26.5	33	20				.2	
5b	92.0	0.004	0.85	2.21	0.075	4.8	0.047		0.011	0.008	267
			7.8	28.7	1.0	62			.14	.10	
6a	98.9	0.002	0.35	0.395	0.032	0.31	0.039			0.003	56
			26	39	3.2	31				.3	
6b	93.8	0.003	0.67	1.74	0.043	3.59	0.015		0.005	0.006	163
			8.5	29.5	.7	61			.08	.10	

(a) Blank entries are below detection limits.

(b) Measurements for ammonia are for the gas phase only and do not include ammonia dissolved in the liquid phase.

Table 19. Gas Generation Rates from Low-Dose Radiolytic Treatment of Tank S-106 Material

	60°C Gas Generation Rates, mol/kg/day								
Run	N_2	N_2O	H_2	NH_3[(a)]	NO_x	CH_4	$C_2H_{2,4,or\,6}$	Other HC[(b)]	Total
1a	1.8E-6	9.8E-7	2.3E-6			1.6E-7			5.2E-6
1b	2.8E-6	3.8E-7	2.7E-6			1.7E-7			6.0E-6
2a	4.0E-6	1.2E-6	2.0E-6			1.0E-7			7.3E-6
2b	3.1E-6	4.9E-7	2.6E-6			1.5E-7			6.3E-6

	90°C Gas Generation Rates, mol/kg/day								
Run	N_2	N_2O	H_2	NH_3[(a)]	NO_x	CH_4	$C_2H_{2,4,or\,6}$	Other HC[(b)]	Total
3a	1.2E-5	2.3E-6	1.7E-5			4.5E-6			3.5E-5
3b	1.1E-5	5.2E-6	1.7E-5			4.7E-6		5.2E-8	3.9E-5
4a	8.0E-6	4.2E-6	1.6E-5			4.2E-6	1.3E-7	8.7E-8	3.2E-5
4b	5.3E-6	1.1E-6	1.6E-5			4.2E-6		4.7E-8	2.6E-5

	120°C Gas Generation Rates, mol/kg/day								
Run	N_2	N_2O	H_2	NH_3[(a)]	NO_x	CH_4	$C_2H_{2,4,or\,6}$	Other HC[(b)]	Total
5a	6.5E-5	1.1E-4	8.6E-5			6.7E-5	7.1E-7	4.8E-7	3.3E-4
5b	3.1E-5	3.8E-6	1.1E-4		5.6E-7	2.5E-4	4.1E-7	2.6E-7	3.9E-4
6a	6.9E-5	8.3E-6	1.0E-4			8.0E-5	7.8E-7	5.2E-7	2.6E-4
6b	4.5E-5	3.8E-6	1.5E-4		4.4E-7	3.2E-4	5.3E-7	3.6E-7	5.2E-4

(a) Measurements for ammonia are for the gas phase only and do not include ammonia dissolved in the liquid phase.
(b) Hydrocarbons.

Table 20. G-values for Gas Generation from S-106 Waste

	H_2	N_2	CH_4
60°C Low Dose Rate	0.014(3)	0.03(1)	0.0007(6)
60°C High Dose Rate	0.0047(6)	0.0048(7)	0.0030(6)
90°C Low Dose Rate	0.10(1)		
90°C High Dose Rate	0.03(1)		
120°C Low Dose Rate	0.5(1)		
120°C High Dose Rate	0.12(2)		

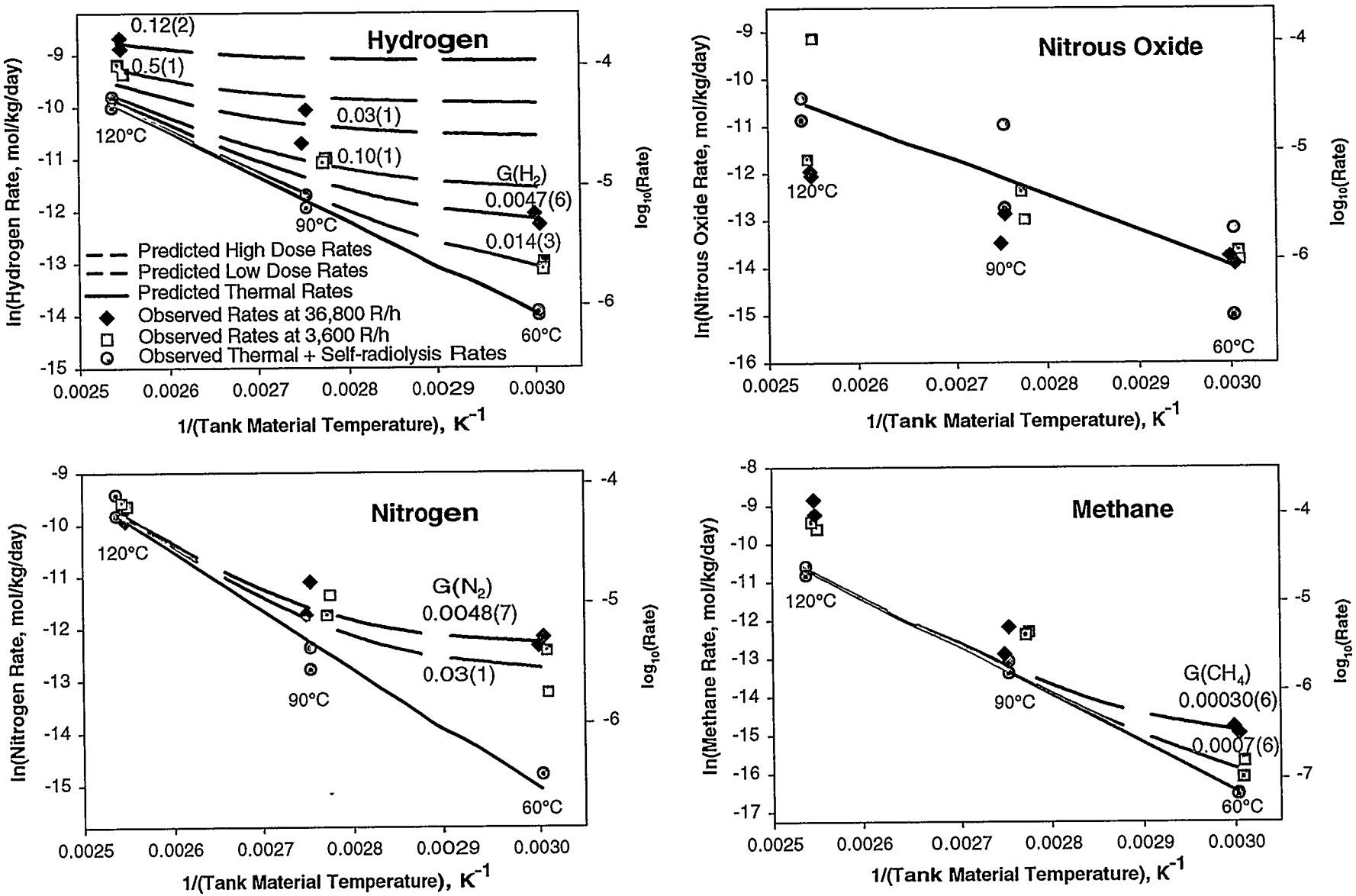

Figure 15. Tank S-106 Gas Generation Rates. The small dot in the center of the symbols distinguishes between duplicate runs.

5.0 S-102 Long-Term Gas Generation Test

Most of the gas generation parameters that we have reported have been obtained at temperatures and dose rates higher than actual tank conditions. To determine how well these parameters apply to tank conditions, a long-term gas generation test was conducted using S-102 material under thermal and radiolytic conditions that closely match the tank temperature (41°C) and dose-rate (207 R/h). The rates obtained from this long-term test are compared with rates predicted using parameters previously obtained at higher temperatures and dose rates (King et al. 1997).

A reaction vessel holder was built to provide approximately the desired dose rate (Figure 16). The dose rate received by the tank material within the vessels was 286 R/h, which is the sum of the external gamma dose rate from the ^{137}Cs source (measured using Fricke dosimetry) and the material's self-dose rate. The S-102 test material, described in King et al. (1997), had lost some water during storage. The weight percent water was determined by thermal gravimetric analysis (TGA) of the material and compared with the weight percent water by TGA given in the *Tank Characterization Report* (Eggers 1996) to determine how much water to add to return the material to its original condition. Two reaction vessels containing the rehydrated S-102 material were placed in the holder. The temperature was maintained at 41°C. The cover gas for this experiment was helium. Three consecutive gas generation runs were made, lasting 40, 37, and 37 days, respectively. The composition of the gas sampled at the end of these runs is listed in Table 21.

In Table 21, hydrogen makes up 40 to 60% of the gas that is produced, except in run 2c, where it is only 7%. This occurs because sample 2c contains 0.3% ammonia, which means that 83% of the gas formed is ammonia. The amount of ammonia in these samples is near the detection limit of 0.1%. This detection limit is relatively high, meaning that, when the ammonia level is deemed detectable, the percent hydrogen is reduced drastically, as it was in sample 2c.

The gas generation rates are listed in Table 22. Under these conditions, the rate of nitrogen production was too slow to detect above atmospheric contamination. Likewise, methane was detected in only three of the six gas samples. The average rates of hydrogen and nitrous oxide gas generation at 286 R/h are also given in Table 22.

The dose rate in this experiment is only 28% higher than the dose rate in the tanks. The gas generation parameters from the short-term experiment can be used to correct the dose rate to tank conditions. Under the long-term experimental conditions, 35% of the hydrogen gas is produced radiolytically; the rest is formed thermally. Fifty-three percent of the nitrous oxide is produced radiolytically. Using these percents, the long-term experimental rates can be corrected to tank conditions, 207 R/h. Under tank conditions, the hydrogen generation rate is 1.9E-7 ± 0.5E-7 mol/kg/day, and the nitrous oxide rate is 2.8E-7 ± 0.6E-7 mol/kg/day (uncertainties represent 95% confidence intervals). This hydrogen rate may be compared with an estimate based on the dome space ventilation system of 9.5E-7 mol/kg/day.[a] These rates are plotted in Figure 17 along with the rates predicted at 207 R/h using parameters from the short-term

(a) Barton B. 1997. Personal communication.

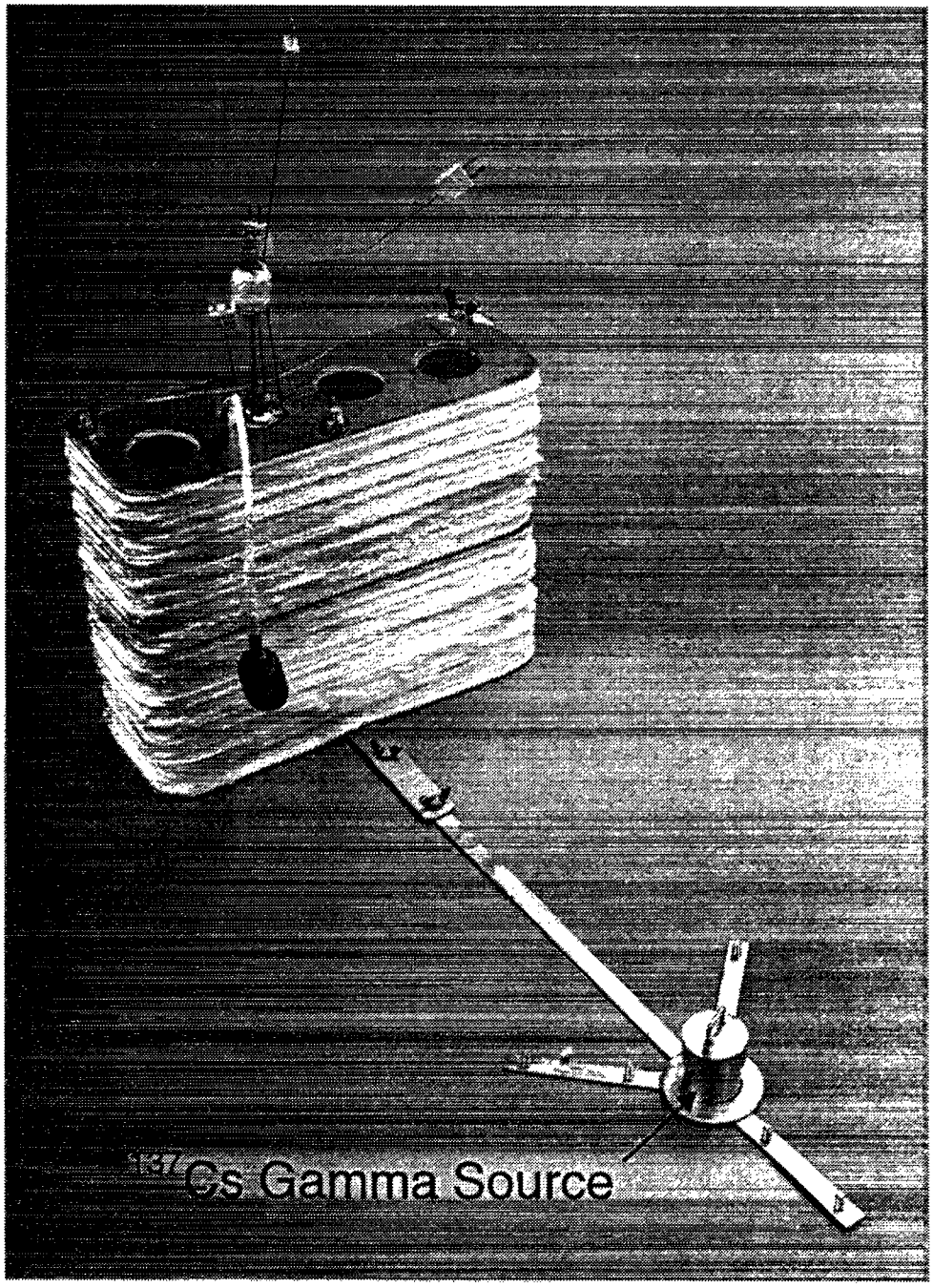

Figure 16. Vessel Holder Used in Long-Term Reaction Experiment. The ^{137}Cs source is shown in the holder in the foreground. The apparatus can accommodate four reaction vessels simultaneously.

experiment. The 95% confidence intervals for the short-term prediction and the long-term observation overlap, indicating that the parameters from the short-term experiment may be used to predict gas generation rates at tank conditions.

Table 21. Mole Percent Composition of Radiolytic Gas Sampled (including He) and Formed (shaded), and Heating Times of Duplicate Systems in Long-Term Test of S-102 Material[(a)]

	Mole Percent of Gas Formed at 41°C										
Run	He	Ar	N_2	H_2	N_2O	CH_4	O_2	NH_3[b]	NO_x	$C_2H_{2,4,\text{ or }6}$	Time, h
1a	99.63	0.004	0.252	0.035	0.027	0.021	0.026				978
			1.42	42	32	25					
1b	99.54	0.006	0.371	0.026	0.022		0.028				906
				54	46						
1c	99.7	0.004	0.195	0.025	0.025	0.002	0.027				886
				48	48	4					
2a	99.47	0.006	0.364	0.046	0.022	0.012	0.071				978
				57	27	15					
2b	99.57	0.006	0.317	0.029	0.017		0.059				906
				63	37						
2c	99.3	0.005	0.26	0.026	0.035		0.069	0.3			886
				7.2	9.7			83			

(a) Blank entries are below detection limits.

Table 22. Gas Generation Rates from Long-Term 41°C Radiolytic Treatment of Tank S-102 Material

	41°C Gas Generation Rates, mol/kg/day				
Run	N_2O	H_2	NH_3	CH_4	Total
1a	3.2E-7	4.1E-7		2.5E-7	9.9E-7
1b	2.8E-7	3.3E-7			1.3E-8
1c	3.3E-7	3.3E-7		2.6E-8	6.9E-7
2a	2.4E-7	5.1E-7	1.1E-8	1.3E-7	3.0E-7
2b	2.1E-7	3.5E-7			5.6E-7
2c	4.4E-7	3.3E-7	3.8E-6		3.6E-6
Average	3.0E-7	3.8E-7			

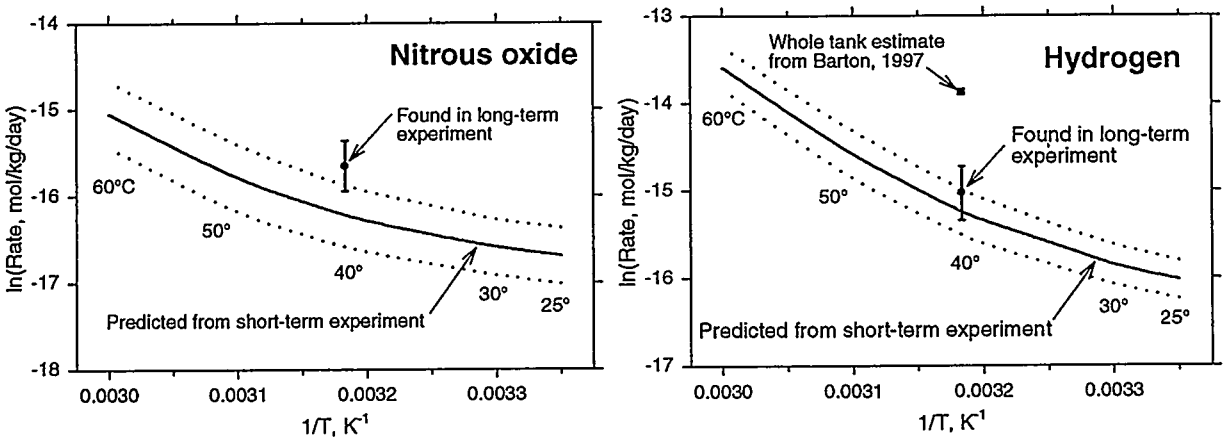

Figure 17. Comparison of Observed Rates under Tank Conditions with Rates Predicted with Parameters from the Short-Term Experiment. The dotted line represents a 95% prediction confidence interval.

6.0 Summary

This report summarizes progress made in evaluating mechanisms by which flammable gases are generated in Hanford single-shell tank wastes based on the results of laboratory tests using actual waste from the convective layer of Tank U-103. Gas generation from U-103 waste samples was first measured with externally applied heat, then with externally applied heat and radiation (^{137}Cs capsule).

The objective of this work was to establish the composition of gaseous degradation products formed in actual tank wastes by thermal and radiolytic processes as a function of temperature. The gas generation tests on Tank U-103 samples focused first on the effect of temperature on the composition and rate of gas generation. Generation rates of nitrogen, nitrous oxide, methane, and hydrogen increased with temperature, and the composition of the product gas mixture varied with temperature.

Arrhenius treatment of the rate data yielded activation parameters for gas generation. The measured thermal activation energies, E_a, were determined to be 91 ± 24 kJ/mol for hydrogen, 108 ± 22 kJ/mol for nitrous oxide; 88 ± 34 kJ/mol for nitrogen; and 156 ± 8 kJ/mol for methane (the uncertainties represent 95% confidence intervals).

The second phase of this work concerned gas generation in the presence of a 36,000 rad/hr (^{137}Cs) external gamma source. The effect of radiation was examined at 40, 60, and 90°C. The best estimates of radiolytic G-values, in molecules per 100 eV, were determined to be 0.0019 ± 0.0003 for nitrous oxide, 0.012 ± 0.003 for nitrogen, and 0.0022 ± 0.0003 for methane. The hydrogen G-value was temperature-dependent, being 0.006 at 40°C and 0.017 ± 0.004 at 60°C. This is the third tank studied in which the G-values were found to be temperature-dependent.

The rate of hydrogen generation under tank conditions (28.7°C, 449 R/h, 3.02E+6 kg waste) was estimated using the thermal and radiolytic activation parameters for gas generation in actual tank waste. The radiolytic generation rate for hydrogen was determined to be 7.1E-8 mol/kg/day, and the thermal rate was 8.7E-8 mol/kg/day. This translates to a total of 0.48 moles of hydrogen generated per day from this tank. This value is much lower than the 5.3 mol/day steady-state hydrogen generation rate reported by McCain (1998) based on Tank U-103 headspace measurements.

The results of low dose-rate tests on AW-101 and S-106 tank material are also presented. $G(H_2)$ appears to be dose rate-dependent at 60°C. The ratio of low to high dose-rate G-values is 2.1 ± 0.1 for AW-101 material, and 3.0 ± 0.9 for S-106 material. $G(H_2)$ also appears to be temperature-dependent. The ratio of 90°C to 60°C high dose-rate G-values is 3.6 ± 0.7 for AW-101 material, 6 ± 4 for S-106 material, and 4.7 ± 1.2 for U-103 material.

The results of a long-term test on S-102 material, maintained near tank temperature and tank dose rate, are also presented. The observed rates agree within experimental error with rates predicted using rate parameters obtained at higher temperatures and dose rates, indicating that rate parameters obtained at higher temperatures and dose rates are applicable to tank conditions.

7.0 References

Briesmeister JF. March 1997. *MCNP—A General Monte Carlo N-Particle Transport Code.* LA-12625-M, Los Alamos National Laboratory, Los Alamos, New Mexico.

Bryan SA and LR. Pederson. 1995. *Thermal and Combined Thermal and Radiolytic Reactions Involving Nitrous Oxide, Hydrogen, and Nitrogen in the Gas Phase; Comparison of Gas Generation Rates in Supernate and Solid Fractions of Tank 241-SY-101 Simulated Wastes.* PNL-10490, Pacific Northwest Laboratory, Richland, Washington.

Bryan SA, LR Pederson, CM King, SV Forbes, and RL Sell. 1996. *Gas Generation from Tank 241-SY-103 Waste.* PNL-10978, Pacific Northwest National Laboratory, Richland, Washington.

Carlson CD. February, 1997. *Speciation of Organic Carbon in Hanford Waste Storage Tanks: Part 1.* PNNL-11480, Pacific Northwest National Laboratory, Richland, Washington.

Eggers RF. 1996. *Tank Characterization Report for Single-Shell Tank 241-S-102.* WHC-SD-WM-ER-611, Westinghouse Hanford Company, Richland, Washington.

Johnson GD, WB Barton, RC Hill, JW Brothers, SA Bryan, PA Gauglitz, LR Pederson, CW Stewart, and LH Stock. 1997. *Flammable Gas Project Topical Report.* HNF-SP-1193 Rev. 2, Lockheed Martin Hanford Corp., Richland, Washington.

King CM, LR Pederson, and SA Bryan. 1997. *Thermal and Radiolytic Gas Generation from Tank 241-S-102 Waste.* PNNL-11600, Pacific Northwest National Laboratory, Richland, Washington.

Laidler KJ. 1987. *Chemical Kinetics, 3rd Ed.* Harper and Row, New York.

McCain DJ and RE Bauer. 1998. *Results of Vapor Space Monitoring of Flammable Gas Watch List Tanks.* HNF-SD-WM-TI-797 Rev 3, Lockheed Martin Hanford Corp., Richland, Washington.

Pederson LR and SA Bryan. 1996. *Status and Integration of Studies of Gas Generation in Hanford Wastes.* PNNL-11297, Pacific Northwest National Laboratory, Richland, Washington.

Person JC. 1996. *Effects of Oxygen Cover gas and NaOH Dilution on Gas Generation in Tank 241-SY-101 Waste.* WHC-SD-WM-DTR-043, Westinghouse Hanford Company, Richland, Washington.

Sasaki LM, SR Wilmarth, and TT Tran. 1998. *Tank Characterization Report for Single-Shell Tank 241-U-103.* HNF-SD-WM-ER-71 Rev. 1, Lockheed Martin Hanford Corp., Richland, Washington.

Spinks JTW and RJ Woods. 1990. *An Introduction to Radiation Chemistry.* John Wiley and Sons, New York.

Distribution

No. of Copies

Offsite

2 DOE Office of Scientific and Technical Information

H. Babad
2540 Cordoba Court
Richland, WA 99352

D. Campbell
102 Windham Road
Oak Ridge, TN 37830

P. DíEntremont
Westinghouse Savannah River Co.
703-H
Aiken, SC 29802

C. W. Forsberg
Oak Ridge National Laboratory
P.O. Box 2008, MS-6495
Oak Ridge, TN 37831-6495

B. C. Hudson
P.O. Box 271
Lindsborg, KS 67456

J. L. Kovach
P.O. Box 29151
70000 Huntley Road
Columbus, OH 43229

T. S. Kress
102-B Newridge Road
Oak Ridge, TN 37830

K. Lang
1041 Cloverleaf Bldg.
1900 Germantown Rd
Germantown, MD 20874

No. of Copies

T. E. Larson
2711 Walnut St.
Los Alamos, NM 87545

Los Alamos National Laboratory
P.O. Box 1663
Los Alamos, NM 87545
Attn: W.L. Kubic K575

D. Meisel
341 Radiation Laboratory
University of Notre Dame
Notre Dame, IN 46556-0679

D. A. Powers
Sandia National Laboratories
MS-0744
Albuquerque, NM 87185-0744

Scott E. Slezak
806 Hermosa NE
Albuquerque, NM 87110

Onsite

2 DOE Richland Operations Office

C. A. Groendyke	S7-54
G. W. Rosenwald	S7-54

25 Hanford Contractors

S. A. Barker	R2-11
W. B. Barton	R2-12
R. E. Bauer	G1-54
R. J. Cash	S7-73
A. F. Choho	R3-73
K. A. Gasper	A3-03

No. of Copies

J. M. Grigsby	R1-49
D. L. Herting	T6-09
K. M. Hodgson	R2-11
T. A. Hu	R2-11
J. R. Jewett	R3-73
G. D. Johnson (5)	S7-73
N. W. Kirch	R2-11
C. E. Leach	R1-49
J. W. Lentsch	S5-07
J. E. Meacham	R1-49
M. A. Payne	R2-58
J. C. Person	T6-07
R. E. Raymond	G1-54
D. A. Reynolds	R2-11
L. M. Stock	S7-73

No. of Copies

34 Pacific Northwest National Laboratory

J. M. Bates	K7-15
S. Q. Bennett	K7-90
P. R. Bredt	P7-25
J. W. Brothers (5)	K9-20
S. A. Bryan (5)	P7-25
S. V. Forbes	P7-25
P. A. Gauglitz	K6-28
J. L. Huckaby	K6-80
C. M. King (5)	P7-25
W. L. Kuhn	K7-15
L. A. Mahoney	K7-15
P. A. Meyer	K7-15
L. R. Pederson	K2-44
L. M. Peurrung	K6-24
S. D. Rassat	K6-28
C. W. Stewart	K7-15
W. C. Weimer	P7-27
Information Release (5)	K1-06